NAVAL POSTGRADUATE SCHOOL
Monterey, California

OTIC
ELECTE
MAY 3 0 1989
D

THESIS

RADAR CROSS SECTION OF A PLANAR
FRACTAL TREE

by

John Demiris

March 1989

Thesis Advisor: Ramakrishna Janaswamy

REPORT DOCUMENTATION PAGE

1a. REPORT SECURITY CLASSIFICATION UNCLASSIFIED	1b. RESTRICTIVE MARKINGS
2a. SECURITY CLASSIFICATION AUTHORITY	3. DISTRIBUTION/AVAILABILITY OF REPORT
2b. DECLASSIFICATION/DOWNGRADING SCHEDULE	Approved for public release; distribution is unlimited

4. PERFORMING ORGANIZATION REPORT NUMBER(S)	5. MONITORING ORGANIZATION REPORT NUMBER(S)

6a. NAME OF PERFORMING ORGANIZATION Naval Postgraduate School	6b. OFFICE SYMBOL (If applicable) 52	7a. NAME OF MONITORING ORGANIZATION Naval Postgraduate School
6c. ADDRESS (City, State, and ZIP Code) Monterey, California 93943-5000		7b. ADDRESS (City, State, and ZIP Code) Monterey, California 93943-5000

8a. NAME OF FUNDING/SPONSORING ORGANIZATION	8b. OFFICE SYMBOL (If applicable)	9. PROCUREMENT INSTRUMENT IDENTIFICATION NUMBER

8c. ADDRESS (City, State, and ZIP Code)	10. SOURCE OF FUNDING NUMBERS			
	PROGRAM ELEMENT NO.	PROJECT NO.	TASK NO.	WORK UNIT ACCESSION NO.

11. TITLE (Include Security Classification)

RADAR CROSS SECTION OF A PLANAR FRACTAL TREE

12. PERSONAL AUTHOR(S)
DEMIRIS, JOHN

13a. TYPE OF REPORT Master's Thesis	13b. TIME COVERED FROM _____ TO _____	14. DATE OF REPORT (Year, Month, Day) 1989 March	15. PAGE COUNT 97

16. SUPPLEMENTARY NOTATION
The views expressed in this thesis are those of the author and do not reflect the official policy or position of the Department of Defense or U.S. Govt.

17	COSATI CODES		18 SUBJECT TERMS (Continue on reverse if necessary and identify by block number)
FIELD	GROUP	SUB-GROUP	Radar Cross Section, Fractal Tree, Moment Method

19 ABSTRACT (Continue on reverse if necessary and identify by block number)

Electromagnetic scattering from trees and vegetation is of prime importance in radar and remote sensing. The actual problem of scattering from trees is rather complicated and involves three dimensional scattering from lossy, electrically large, and randomly oriented objects. In this thesis, the radar cross section of a planar fractal tree is considered. Although a planar tree is far from being real, scattering from it sheds light on the scattering phenomenon from an actual tree. The planar tree is generated using fractal geometry and its branches are considered perfectly conducting. The tree is illuminated by a plane wave and the problem is solved using the moment method. Data is presented for the radar cross section for different branching angles of the tree and at different frequencies.

20 DISTRIBUTION/AVAILABILITY OF ABSTRACT ☒ UNCLASSIFIED/UNLIMITED ☐ SAME AS RPT ☐ DTIC USERS	21 ABSTRACT SECURITY CLASSIFICATION UNCLASSIFIED	
22a NAME OF RESPONSIBLE INDIVIDUAL Ramakrishna Janaswamy	22b TELEPHONE (Include Area Code) (408) 646-3217	22c OFFICE SYMBOL 62Js

DD FORM 1473, 84 MAR — 83 APR edition may be used until exhausted — SECURITY CLASSIFICATION OF THIS PAGE
All other editions are obsolete

☆ U.S. Government Printing Office: 1986—606-24.

i

Radar Cross Section of a Planar
Fractal Tree

by

John Demiris
Lieutenant, Hellenic Navy
B.S., Hellenic Naval Academy, 1979

Submitted in partial fulfillment of the
requirements for the degree of

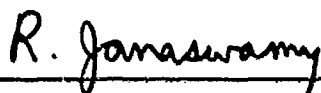## MASTER OF SCIENCE IN ELECTRICAL ENGINEERING
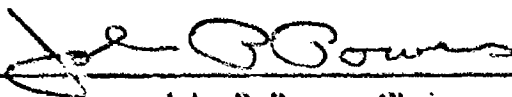
from the

NAVAL POSTGRADUATE SCHOOL
March 1989

Author: _____

John Demiris

Approved by: _____

Ramakrishna Janaswamy, Thesis Advisor

_____

Michael A. Morgan, Second Reader

_____

John P. Powers, Chairman,
Department of Electrical and Computer Engineering

_____

Gordon E. Schacher,
Dean of Science and Engineering

ABSTRACT

Electromagnetic scattering from trees and vegetation is of prime importance in radar and remote sensing. The actual problem of scattering from trees is rather complicated and involves three dimensional scattering from lossy, electrically large, and randomly oriented objects.

In this thesis, the radar cross section of a planar fractal tree is considered. Although a planar tree is far from being real, scattering from it sheds light on the scattering phenomenon from an actual tree. The planar tree is generated using fractal geometry and its branches are considered perfectly conducting. The tree is illuminated by a plane wave and the problem is solved using the moment method. Data is presented for the radar cross section for different branching angles of the tree and at different frequencies.

Accession For	
NTIS CRA&I	☑
DTIC TAB	☐
Unannounced	☐
Justification	
By	
Distribution /	
Availability Codes	
Dist	Avail and/or Special
A-1	

TABLE OF CONTENTS

AKNOWLEDGEMENTS

I would like to express my thanks to Professor Ramakrishna Janaswamy, my thesis advisor, for his experienced guidance and great assistance in this study. I also express my thanks to Professor T.R. Nelson of University of California, San Diego, for providing the program that generates the planar fractal trees.

I would also like to dedicate this thesis to my wife Maria and my son Stratis for their continuing support, love, understanding, and patient help throughout my stay at the Naval Postgraduate School.

Finally, I wish to thank all the Greek tax-payers, for having paid the expenses for my course of study.

I. INTRODUCTION

A. NEED FOR THE STUDY

The trees existing in the natural world are fractal anisotropic. They are made up of long, intersecting and lossy objects. The geometry of these objects is not easy to set up as they are randomly oriented in a three dimensional space. The use of fractals facilitates the modeling of semi–randomly distributed structures. Mandelbrodt [Ref. 1] has shown that a number of naturally occurring phenomenon such as coastlines, clouds, trees, etc. are fractal in nature. For instance, when a branch is divided into two (or more), the ratio of the length of the subbranches to the main branch length remains constant. Furthermore, the branching angle also remains the same.

In this thesis, scattering from planar fractal trees is considered. The radar cross section of a real fractal tree is a complicated scattering problem. The analysis of this problem in a two dimensional space gives an approximate idea of the radar cross section of a real tree.

The radar cross section of an object is a quantitative measure of the ratio of the power density that is received and scattered by the object to the power density of the electromagnetic wave that illuminates that object. The radar cross section is independent of the range of the object for the far–field situation. The theoretical definition of the radar cross section "σ" is given by the formula:

$$\sigma = 4\pi R^2 \lim_{R \to \infty} \left| \frac{E^s}{E^i} \right|$$

where $\hat{E}^i$ is the incident electric field vector, $\hat{E}^S$ is the scattered electric field vector, and R is the distance between the scattered object and the point of observation. The radar cross section has dimensions of area. Usually, it is expressed in square wavelengths.

B. STATEMENT OF THE PROBLEM

This thesis investigates the radar cross section of planar fractal trees. These trees are composed of planar thin strip dipoles of arbitrarily dimensions and orientations in a plane. These structures are excited by plane waves of various frequencies.

The first step in solving the problem is to calculate the induced current distribution on each strip. The calculation of the current distribution is based on the theory of the moment method and requires a knowledge of the impedance between any two of these strips as well as the voltage on each planar strip due to the incident electric field. The basic concepts and the calculation of the current distribution are described in Chapter 2.

In Chapter 3, the development of a FORTRAN program, is presented. The evaluation of the radar cross section requires the knowledge of the scattered electric field due to the induced currents on the planar strips. The program computes the scattered electric field and then the radar cross section of that structure. The details of these calculations are also presented in this Chapter.

The computer models that are used by the developed program are presented in Chapter 4. Their generation is based on the fractal geometry. An existing and modified program is used to generate the geometry of the planar fractal trees in order to be used as input in the developed program.

2

The numerical results of the radar cross section of a single planar dipole and a a number of planar fractal trees are presented in Chapter 5. The scattering from a single dipole is compared with standard results for a similar case. The limitations of the developed program are also presented in this Chapter.

In Chapter 5, the conclusions of the radar cross section results and recommendations are presented. The two programs that are used for this investigation are listed in the Appendices.

II. METHOD OF MOMENTS THEORY

In this section of the study, the basic concepts of the moment method theory are presented. This theory is used in the development of the RCS program to find the current distribution on a planar strip due to an incident plane wave.

For a given structure consisting of planar dipoles the impedance between any two of them is calculated from the knowledge of the geometry and the wavelength of the incident plane wave. The voltage on each dipole is calculated from the knowledge of the characteristics of the incident electric field. The induced current distribution on each dipole of the structure is determined from the calculated impedance and voltage using the method of moments theory.

A. GENERAL THEORY

The method of moments is a numerical procedure for solving integral equations of the form:

$$\int_a^b f(x')K(x,x')dx' = g(x), \quad a < x < b \qquad \text{(eqn 2.1)}$$

where $f(x')$ is an unknown function, $K(x,x')$ is a known Kernel or Green's function, and $g(x)$ is a given function. This procedure reduces the integral equation (eqn 2.1) to a system of simultaneous linear algebraic equations in terms of some unknown coefficients. This method requires that the function $f(x')$ be approximated by a series of N expansion functions or " basis functions ", such that

$$f(x') \approx \sum_{n=1}^{N} a_n f_n(x'), \qquad n=1,2,......,N \qquad \text{(eqn 2.2)}$$

where the domain of $f_n(x')$ is the same as that of $f(x')$ and a_n's are the complex unknown expansion coefficients.

There are two types of basis functions. The subdomain functions, which are nonzero over a part of the domain of the unknown function $f(x')$, and entire domain functions being nonzero over the entire domain of $f(x')$. In antennas, some commonly employed subdomain basis functions are the piecewise sinusoid functions, the unit height—pulse functions and the piecewise triangular functions.

The subdomain procedure requires subdivision of the structure into N nonoverlapping segments. Figure 2.1 shows a segmented line where the segments are assumed to be collinear and of equal length, although this condition is not necessary.
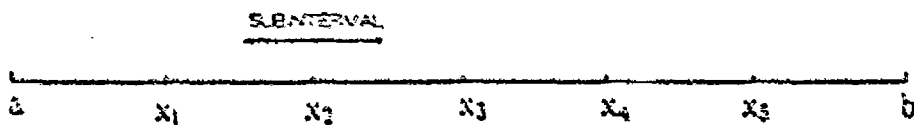
SUBINTERVAL

a x_1 x_2 x_3 x_4 x_5 b

Figure 2.1 Segmented Line. [From Ref. 2]

Figure 2.2 shows a subdomain unit height—pulse function which produces a staircase representation of the unknown function $f(x')$. Figure 2.3 shows a subdomain sinusoid basis function and the representation of the function $f(x')$. Figure 2.4 shows a subdomain triangular basis function producing a smoother representation of the function $f(x')$ than the case of the unit height—pulse basis function.

The use of entire—domain basis functions does not require any segmentation of the structure. One of the most most commonly used basis functions of this kind is the sinusoidal basis functions.
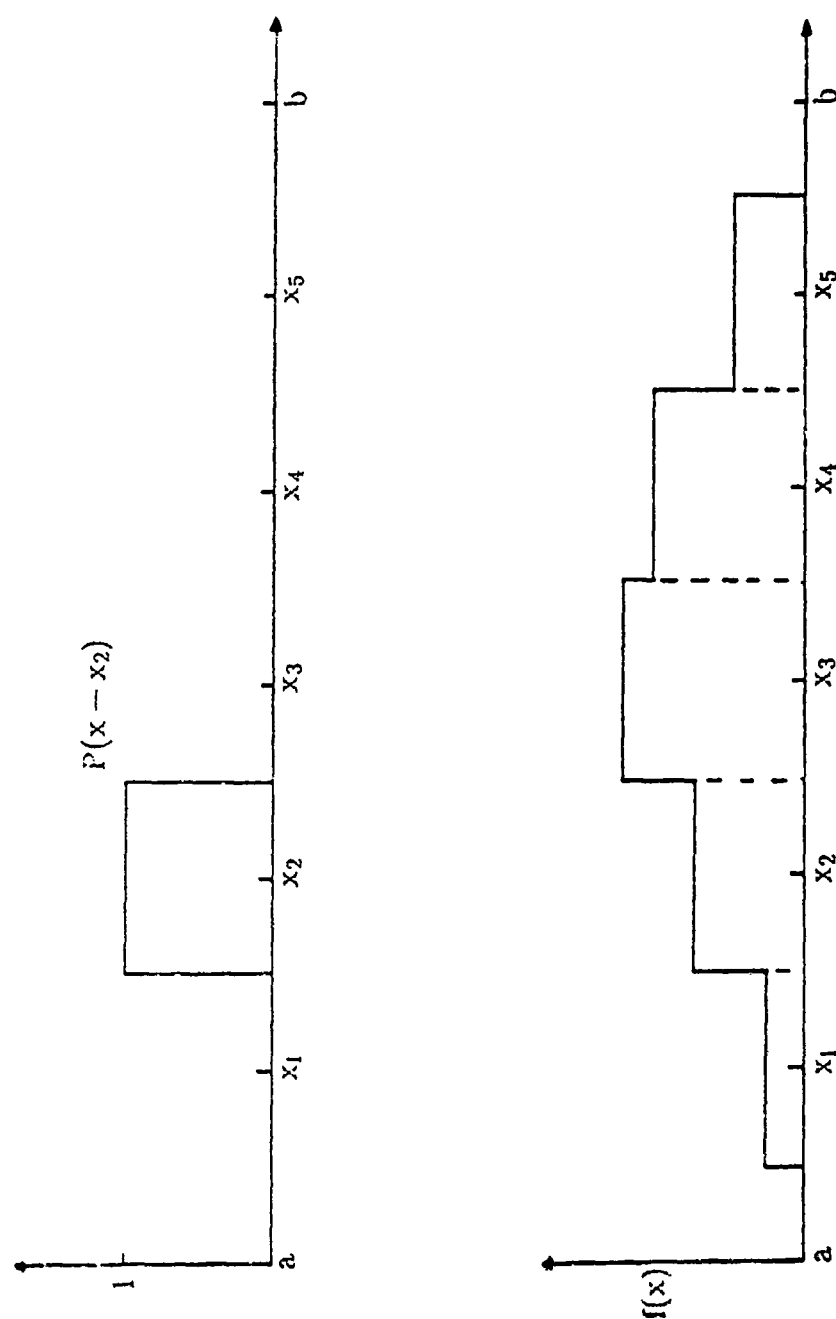
Figure 2.2 Unit Height—Pulse Basis Function and a Staircase Representation of $f(x')$. [From Ref. 2]
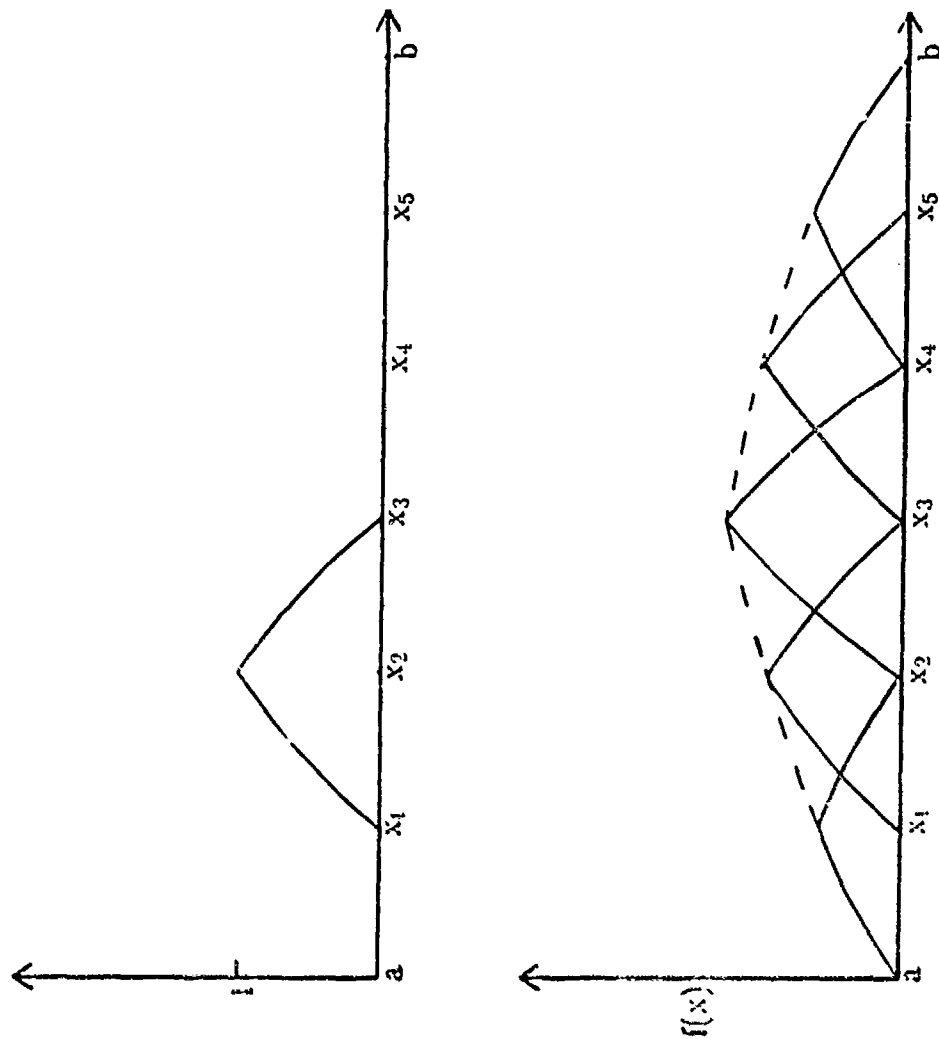
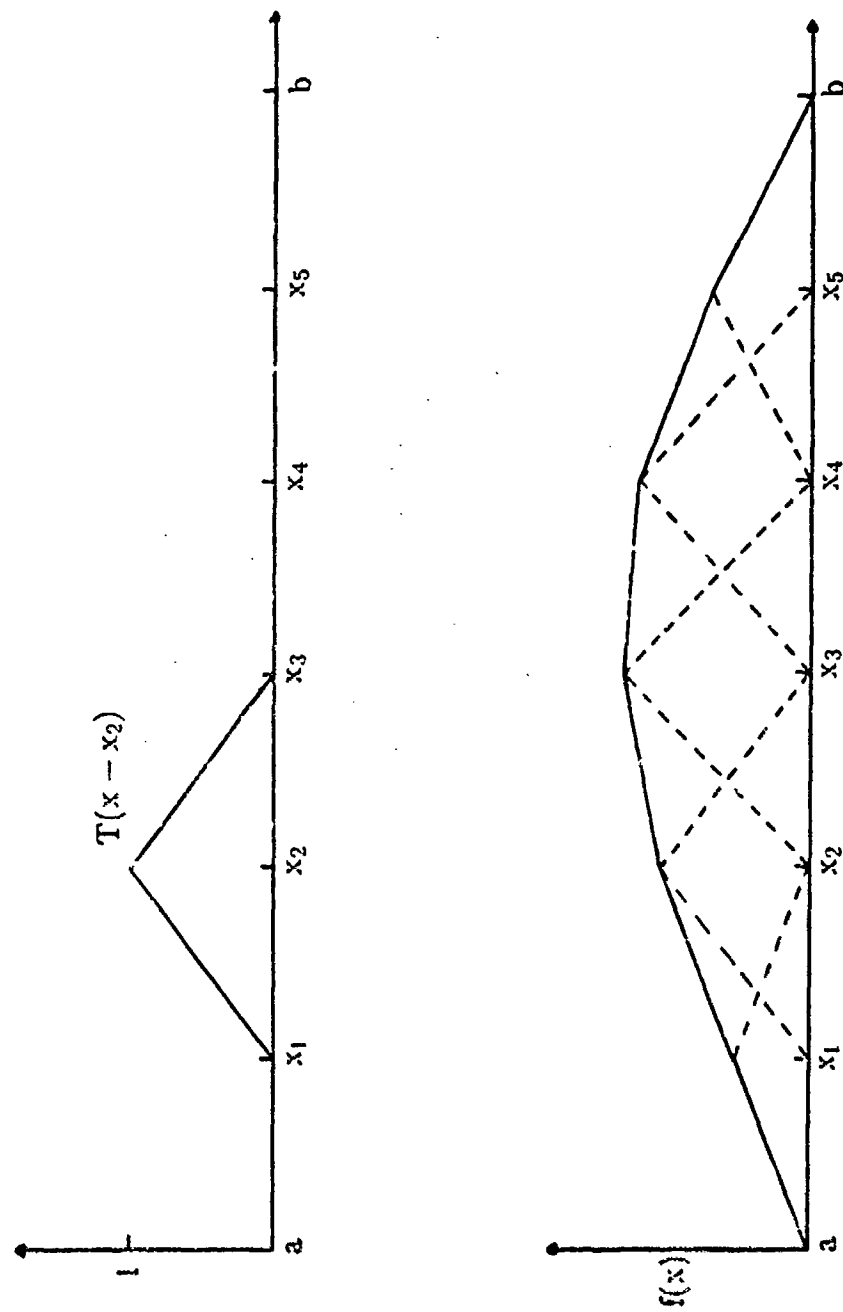Figure 2.3 Sinusoid Basis Function and a Representation

of f(x'). [From Ref. 3]

8

Figure 2.4 Triangular Basis Function and a Representation
of $f(x')$. [From Ref. 2]

9

The substitution of the function $f(x')$ by a sequence of N basis functions leads to one equation of N unknowns of the expansion coefficients a_n, which can be found by using N linearly independent equations. These equations are set up by the use of "testing or weighting" functions $\omega_m(x)$, m=1,2,....N. At this point the definition of the inner product is required. The inner product $\langle f, g \rangle$ between any two functions or vectors f, g is a scalar operation defined as

$$\langle i, g \rangle = \iint_S f \cdot g \, ds \qquad \text{(eqn 2.3)}$$

where S is the surface of the structure that is analyzed [Ref 4]. The inner product of the selected testing functions $\omega_m(x)$, with the two sides of the original integral equation leads to the equation:

$$\left\langle \omega_m(x), \int_a^b f(x')K(x,x')dx' \right\rangle = \left\langle g(x), \omega_m(x) \right\rangle$$

$$\text{(eqn 2.4)}$$

or

$$\left\langle \omega_m(x), \int_a^b \sum_{n=1}^N a_n f_n(x')dx' \right\rangle = \left\langle g(x), \omega_m(x) \right\rangle, \quad m = 1,2,\ldots\ldots,N$$

$$\text{(eqn 2.5)}$$

The use of the above definition for the inner product, yields:

$$\sum_{n=1}^N a_n \int_a^b \omega_m(x)dx \int_a^b f_n(x')K(x,x')dx' = \int_a^b g(x)\omega_m(x)dx, \quad m = 1,2,\ldots\ldots N$$

$$\text{(eqn 2.6)}$$

The following substitutions

$$V_m = \int_a^b g(x)\omega_m(x)dx, \qquad m=1,2,.......,N \qquad \text{(eqn 2.7)}$$

and

$$Z_{mn} = \int_a^b \omega_m(x)dx \int_a^b f_n(x')K(x,x')dx', \qquad m,n=1,2,....N$$

$$\text{(eqn 2.8)}$$

result in a matrix equation of the form:

$$[Z_{mn}]\cdot[a_n] = [V_m] \qquad \text{(eqn 2.9)}$$

The unknowns $[a_n]$ can be obtained through a matrix inversion:

$$[a_n] = [Z_{mn}]^{-1}\cdot[V_m] \qquad \text{(eqn 2.10)}$$

where $[Z_{mn}]^{-1}$ is the inverse matrix. The column vector $[V_m]$ depends upon the given function $g(x)$ and the selected testing functions $\omega_m(x)$. The matrix $[Z_{mn}]$ depends upon the known kernel $K(x,x')$ and both the selected basis and testing functions. Once the expansion coefficients are known, the function $f(x')$ is also known.

The choice of basis and testing or weighting functions is based upon experience and the rule is that their number has to be the same. The procedure of using the same basis and testing functions is called the " Garlekin's method ".

B.   APPLICATIONS TO EM THEORY

A number of problems in electromagnetic radiation and scattering can be solved by the method of moments. In the present case, the simple case of a perfectly conducting object " situated in free space " is considered.

The basic problem is to investigate the case when an object is illuminated by fields of known impressed electric and magnetic currents (J^i, M^i). In the absence of

the object, the impressed currents radiate the assumed known incident electric and magnetic fields (E^i, H^i). In the presence of this object, the impressed currents radiate the unknown total fields (E^t, H^t).

The integral equation is obtained by the surface equivalence principle, replacing the object by free space together with the electric surface current density

$$J = \hat{n} \times H^t \qquad \text{(eqn 2.11)}$$

where J exists on the entire surface S of the object and $\hat{n}$ is the unit vector normal to that surface. In free space, J radiates the scattered fields E^S, H^S

$$E^S = E^t - E^i \qquad \text{(eqn 2.12)}$$

$$H^S = H^t - H^i \qquad \text{(eqn 2.13)}$$

The boundary conditions for this case enforce the total tangential electric field on the surface S to zero:

$$\hat{n} \times (E^S + E^i) = 0 \qquad \text{(eqn 2.14)}$$

This is an integral equation for J since the scattered electric field E^S can be written as an integral over S of the dot product of J and the dyadic free space Green's function. [Ref. 5]

As the geometry of the object is known, it is more convenient to use the total current I instead of the total current density J. So, the problem is to find the unknown current I induced by the incident electric field. The method of moments solve these kind of problems by the following procedure.

The first step is to expand the unknown current I in terms of some basis set:

$$I \approx \sum_{n=1}^{N} I_n F_n \qquad \text{(eqn 2.15)}$$

where the I_n are the sequence of N unknown complex coefficients, and the F_n is a

sequence of N known modes or basis functions. The best choice of F_n for a given problem could be quite involved and is discussed in [Ref. 4, pp 308–310].

The second step is to select the testing or weighting functions ω_m, m=1,2,....N. These can be identical with the basis functions or different. The inner product of the sequence of N weighting functions ω_m, with both sides of the integral equation gives a N x N system of simultaneous linear algebraic equations of the symbolic form:

$$[Z] \cdot [I] = [V] \qquad \text{(eqn 2.16)}$$

where I is the current column vector whose N components give the values of I_n and [Z] is the N x N impedance matrix given by the equation

$$Z_{mn} = -\iint_S E_n^S \cdot \omega_m ds \qquad \text{(eqn 2.17)}$$

where S is the surface of the structure being analyzed. The impedance matrix [Z] is always symmetric, and, for the special case of a thin dipole instead of an arbitrary object, is also a Toeplitz matrix. In a Toeplitz matrix, Z_{mn} depends only on $|m-n|$.

Generally, [Z] is dependent only on the geometry and material composition of the scatterer, but not on the incident fields [Ref 5]. The right–hand side of the last equation is the voltage vector whose N components give the corresponding mode voltage. The voltage vector depends only on the excitation, i.e., the incident electric field. The dimensions of the elements of [Z] and [V] are volt–amps (VA), while the elements of [I] are dimensionless.

The solution of the last matrix equation is the column vector [I], whose elements represent the complex coefficients I_n. As the total current I was expanded by a sequence of N known modes or basis functions and the complex coefficients I_n are known, the total current and so the total current density J is also known.

13

Although the choice of weighting functions is free, it has to be considered that the matrix equation being solved requires the evaluation of N^2 terms and each term requires two or more integrations. When these integrations are to be done numerically, the computations become complicated. There is a way to reduce this complexity by choosing as weighting functions the Dirac delta functions. This is the method of *point—matching* in which delta functions are enforced only at discrete points on the surface S. The results of this method can be quite accurate especially when the discrete points are selected to be equally spaced. The solution satisfies the electromagnetic boundary conditions (e.g., vanishing tangential electric fields on the surface of an electric conductor) only at discrete points [Ref 4]. Between these points the boundary conditions may not be satisfied. In this case it is required to define the deviation as a residual (e.g., residual=$\Delta E|_{tan} = E^S|_{tan} + E^i|_{tan} \neq 0$ on the surface S of an electric conductor) and use the method of weighted residuals so that the boundary conditions will be satisfied in an average sense over the entire surface S.

III. ANALYSIS AND DEVELOPMENT OF RCS PROGRAM

In this chapter, the basic steps that are involved in the calculation of the Radar Cross Section (RCS) of a planar structure composed of conducting strips are presented. As mentioned earlier, the fractal tree is modeled as consisting of planar thin strips. The radar cross section of the fractal tree is calculated using the method of moments. A Fortran program is developed to calculate the RCS of the tree for a specified geometry and at a given frequency.

The moment method discretizes an integral equation to a matrix equation of the form:

$$[Z] \cdot [I] = [V] \qquad \text{(eqn 3.1)}$$

where [Z] is the impedance matrix whose elements represent the mutual impedance between any two dipoles of a given structure depending upon the wavelength and geometry of the structure, [V] is the voltage matrix whose elements correspond to the voltage on each dipole due to excitation (incident electric field), and [I] is the unknown matrix whose elements represent the induced current on each dipole.

A. DEVELOPMENT OF RCS PROGRAM

The numerical results for RCS are obtained from a Fortran program that calculates backscattered RCS of a planar structure consisting of arbitrarily oriented dipoles. For convenience, the structure will be assumed to be in the y–z plane of an xyz cartesian coordinate system.

Figure 3.1 shows the structure to be investigated. A large number of planar dipoles of variable lengths, widths, and orientations in the y–z plane is

illuminated by a plane wave with electric field linearly polarized and characterized by the angles φ_0 and θ_0. It is required to calculate the backscattered RCS from this structure.

The incident electric field $\hat{E}^i$ is given by the formula

$$\hat{E}^i = \hat{e} \cdot e^{-j(k_x \cdot x + k_y \cdot y + k_z \cdot z)} \qquad \text{(eqn 3.2)}$$

where $\hat{k}$ is the propagation vector and

$$k_x^2 + k_y^2 + k_z^2 = k_0^2 = \omega^2 \mu_0 \epsilon_0 \qquad \text{(eqn 3.3)}$$

$$k_0 = \frac{2\pi}{\lambda} \qquad \text{(eqn 3.4)}$$

$$k_x = k_0 \sin\theta_0 \cos\varphi_0 \qquad \text{(eqn 3.5)}$$

$$k_y = k_0 \sin\theta_0 \sin\varphi_0 \qquad \text{(eqn 3.6)}$$

$$k_z = k_0 \cos\theta_0 \qquad \text{(eqn 3.7)}$$

$$\hat{e} = E_x \hat{x} + E_y \hat{y} + E_z \hat{z} \qquad \text{(eqn 3.8)}$$

The electric field $\hat{E}^i$ lies on the plane perpendicular to the direction of propagation of the plane wave. Hence, $\hat{e} \cdot \hat{k} = 0$ implies that

$$E_x k_x + E_y k_y + E_z k_z = 0 \qquad \text{(eqn 3.9)}$$

The substitution of E_y and E_z by the variables a and b (independent variables) gives the coordinate E_x as a dependent variable

$$E_x = -\frac{(ak_y + bk_z)}{k_x} \qquad \text{(eqn 3.10)}$$

Equation 3.1 the becomes

$$\hat{E}^i = \left[a\hat{y} + b\hat{z} - \frac{(ak_y + bk_z)}{k_x}\hat{x} \right] e^{-j(k_x x + k_y y + k_z z)}$$
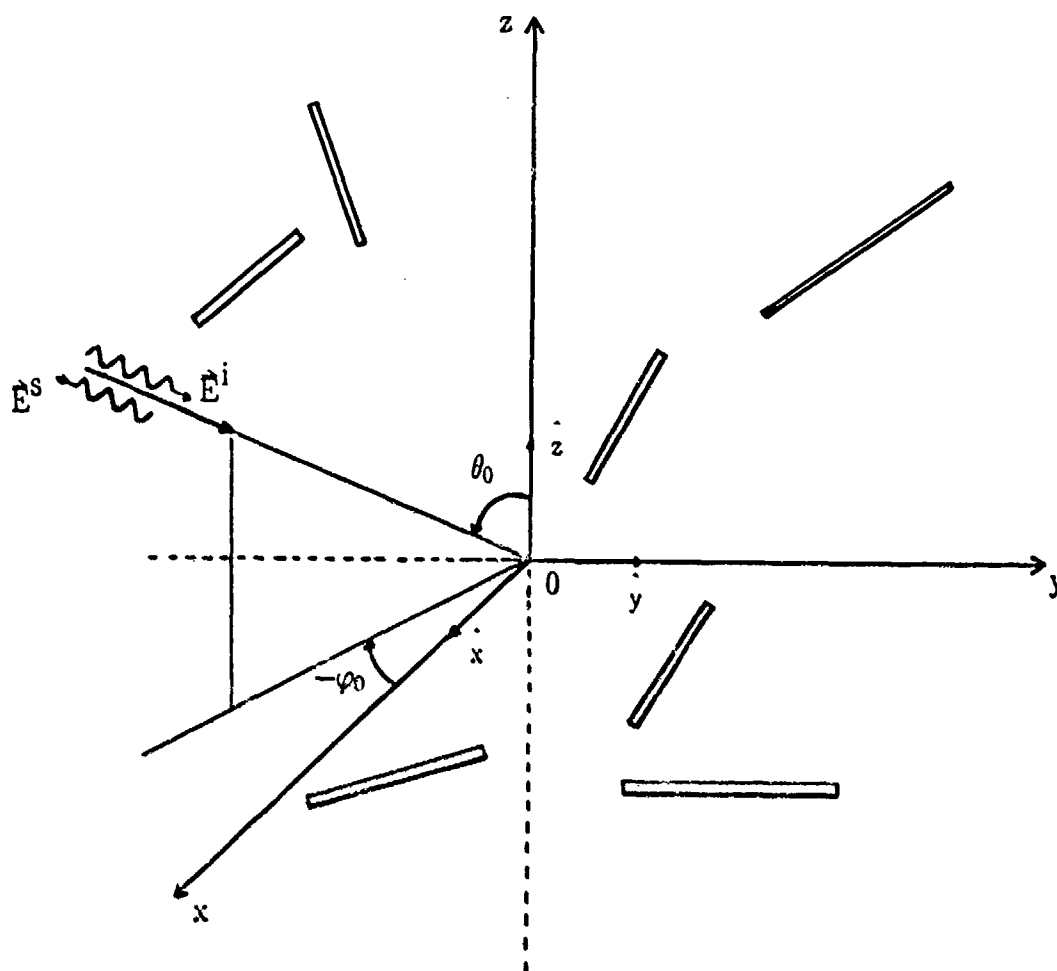
$$\text{(eqn 3.11)}$$

Figure 3.1 Geometry of RCS Program.

The RCS program that has been developed makes the following assumptions:

1. The dipoles are very thin planar strips. The width of the dipoles is assumed to be electrically small so that only the axial current is significant. Further, there is no current variation along the width of the dipoles.

2. The dipoles are not intersecting.

3. The dipoles are perfect conductors.

The program uses the theory of moment method and the way that it solves the problem can be understood if a single planar thin dipole in the y–z plane is considered. Each dipole is subdivided into equal segments. Overlapping Piecewise Sinusoidal (PWS) modes are assumed to exist on the dipole. The length of each PWS mode is equal to the length of two segments. Figure 3.2 shows the m_{th} PWS mode. The PWS mode has a length $2h_m$, and a width $2w_m$. The coordinates of its center are (y_m, z_m), and it is oriented at an angle ψ_m measured from the z axis.

The incident electric field induces current along the axis ζ of that mode. In Figure 3.2, the induced current $\mathbf{J}$ varies sinusoidally along the axis of the m_{th} mode. A new coordinate system η–ζ is introduced, where ζ is the axis of the dipole and η is the axis perpendicular to ζ. The η–ζ coordinate system is obtained by rotating the y–z system about the x–axis through an angle 90°–ψ_m. Figure 3.3 shows the details of this rotation.

The relation between the coordinates of the center of the mode along the axis of the two orthogonal systems is found to be:

$$y = y_m + \zeta \sin(\psi_m) - \eta \cos(\psi_m) \qquad \text{(eqn 3.12)}$$

$$z = z_m + \zeta \cos(\psi_m) + \eta \sin(\psi_m) \qquad \text{(eqn 3.13)}$$

18

The corresponding vector equation is:

$$\dot{y} = \dot{\zeta}\sin(\psi_m) - \dot{\eta}\cos(\psi_m) \qquad \text{(eqn 3.14)}$$

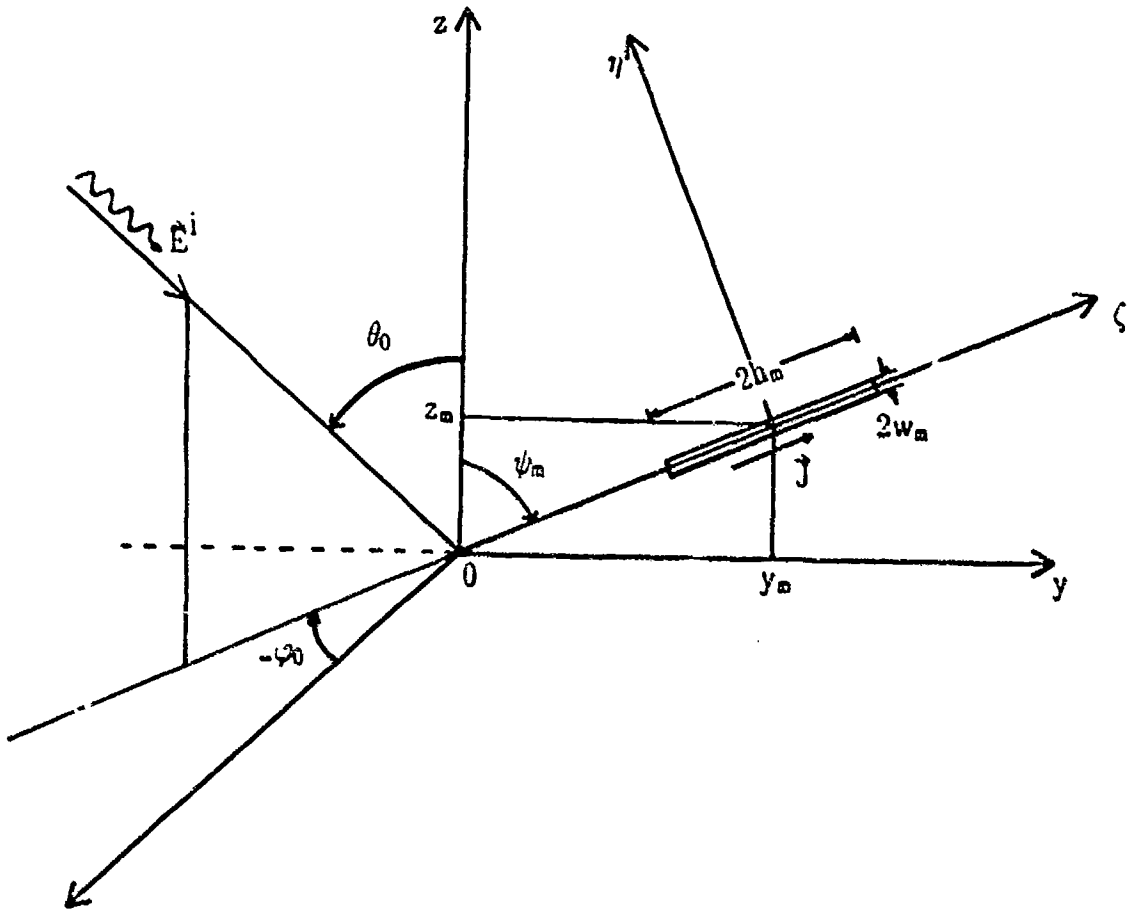$$\dot{z} = \dot{\zeta}\cos(\psi_m) + \dot{\eta}\sin(\psi_m) \qquad \text{(eqn 3.15)}$$

Figure 3.2 Geometry of the m_{th} PWS Mode of the Structure.

19

Figure 3.3 Transformation of PWS Mode's Center Coordinates.

1. Voltage Equations

In this section, expressions for the elements of the voltage matrix [V] due to the incident electric field, are presented. Each element of this matrix corresponds to a PWS mode of the structure that is investigated. The size of the voltage matrix is equal to the total number of modes of the structure.

The induced current density on the m_{th} mode of the structure, due to incident electric field, is

$$\vec{J} = \frac{\vec{\zeta}}{2w_m} \frac{\sin(k_0(h_m - |\zeta|))}{\sin(k_0 h_m)} \qquad \text{(eqn 3.16)}$$

where $2w_m$ is the width and $2h_m$ is the length of the m_{th} mode. For each mode, the induced current variation will be sinusoidal along its axis, being maximum at the center and zero at the end points. The corresponding voltage V_m is

$$V_m = \int_{-\omega_m}^{\omega_m} \int_{-h_m}^{h_m} \vec{E}^i \cdot \vec{J} \,\Big|_{x=0} \, d\zeta d\eta \qquad \text{(eqn 3.17)}$$

From equations 3.11 and 3.16, it is seen that

$$\vec{E}^i \cdot \vec{J} = [a \sin(\psi_m) + b \cos(\psi_m)] \, e^{-j[k_y(y_m + \zeta\sin(\psi_m)) + k_z(z_m + \zeta\cos(\psi_m))]}$$

$$\text{(eqn 3.18)}$$

where ψ_m is the angle between the z axis (reference for angle measurements) and the axis of the mode and y_m, z_m are the coordinates of the center of the mode along the

21

y and z axis respectively. The substitution into equation 3.17, gives the following form of V_m:

$$V_m = \frac{e^{-j(k_y y_m + k_z z_m)}}{\sin(k_0 h_m)} [a \sin(\psi_m) + b \cos(\psi_m)] \int_{-h_m}^{h_m} e^{-jk_\zeta \zeta} \sin(k_0(h_m - |\zeta|)) d\zeta$$

(eqn 3.19)

where $k_\zeta = k_y \sin(\psi_m) + k_z \cos(\psi_m)$. A closed form evaluation of the integral in this equation leads to final form of V_m

$$V_m = \frac{2k_0 V_{om}}{k_\zeta^2 - k_0^2} \left[\cos(k_0 h_m) - \cos(k_\zeta h_m) \right] \qquad k_\zeta \neq \pm k_0$$

(eqn 3.20)

$$V_m = V_{om} h_m \sin(k_0 h_m) \qquad k_\zeta = \pm k_0$$

(eqn 3.21)

where

$$V_{om} = \frac{e^{-j(k_y y_m + k_z z_m)}}{\sin(k_0 h_m)} \left[a \sin(\psi_m) + b \cos(\psi_m) \right]$$

(eqn 3.22)

2. Radiation Equations

In this section, expressions for the far-zone scattered fields due to the m_{th} PWS mode are developed. For far-field observations the electric field is given in spherical coordinates by the following equations [Ref 4]:

$$E_r \approx 0 \qquad \text{(eqn 3.23)}$$

$$E_\theta \approx -\frac{jk_0 e^{-jk_0 r}}{4\pi r}\left(L_\varphi + \eta\, N_\theta \right) \qquad \text{(eqn 3.24)}$$

$$E_\varphi \approx +\frac{jk_0 e^{-jk_0 r}}{4\pi r}\left(L_\theta + \eta\, N_\varphi \right) \qquad \text{(eqn 3.25)}$$

where

$$L_\theta = \iint_S [M_x\cos\theta\cos\varphi + M_y\cos\theta\sin\varphi - M_z\sin\theta]\, e^{+jk_0 r'\cos\psi_m}\, ds'$$

$$\text{(eqn 3.26)}$$

$$L_\varphi = \iint_S [-M_x\sin\varphi + M_y\cos\varphi]\, e^{+jk_0 r'\cos\psi_m}\, ds'$$

$$\text{(eqn 3.27)}$$

$$N_\theta = \iint_S [J_x\cos\theta\cos\varphi + J_y\cos\theta\sin\varphi - J_z\sin\theta]\, e^{+jk_0 r'\cos\psi_m}\, ds'$$

$$\text{(eqn 3.28)}$$

$$N_\varphi = \iint_S [-J_x\sin\varphi + J_y\cos\varphi]\, e^{+jk_0 r'\cos\psi_m}\, ds'$$

$$\text{(eqn 3.29)}$$

$$\eta = 120\pi \qquad \text{(eqn 3.30)}$$

The quantities J_x, J_y, J_z, are the components of the electric current density $\vec{J}_s$ that are induced on the m_{th} mode over the surface S, and the quantities M_x, M_y, M_z, are the coordinates of the magnetic current density $\hat{M}_s$ over the surface S. As the structure is on the y–z plane and $\hat{M}_s$ is zero, the quantities J_x, L_θ, L_φ are zero. Equations 3.24 and 3.25 become:

$$E_\theta \approx \frac{-jk_0 e^{-jk_0 r}\eta}{4\pi r} N_\theta \qquad \text{(eqn 3.31)}$$

$$E_\varphi \approx \frac{+jk_0 e^{-jk_0 r}\eta}{4\pi r} N_\varphi \qquad \text{(eqn 3.32)}$$

As the current density $\vec{J}_m$ is along the ζ–axis, all quantities within the integrals for $\vec{J}$ and $\vec{M}$ will be expressed in terms of the η–ζ system. The surface element that is used in all integrals is ds$'$ = dydz = dζdη = dζ, as the width of the mode is assumed to be very small in terms of its length. The transformations from the y–z system to the ζ–η system are made by using the following substitutions:

$$r'\cos(\psi_m) = y\sin\theta\sin\varphi + z\cos\theta \qquad \text{(eqn 3.33)}$$

where

$$y = y_m + \zeta\sin(\psi_m) \qquad \text{(eqn 3.34)}$$

$$z = z_m + \zeta\cos(\psi_m) \qquad \text{(eqn 3.35)}$$

and

$$\vec{J}_m = J_y\hat{y} + J_z\hat{z} = \hat{\zeta}\left[\frac{I_m}{2w_m\sin(k_0 h_m)}\sin(k_0(h_m - |\zeta|))\right]$$

$$\text{(eqn 3.36)}$$

where

$$J_y = J_\zeta \sin(\psi_m) \qquad \text{(eqn 3.37)}$$

$$J_z = J_\zeta \cos(\psi_m) \qquad \text{(eqn 3.38)}$$

These substitutions and algebraic manipulations give the quantities $N_{\theta m}$ and $N_{\varphi m}$ for the m_{th} mode in the ζ–η system:

$$N_{\theta m} = N_{\theta_0}\frac{-2k_0}{E_m^2 - k_0^2}\left[\cos(E_m h_m) - \cos(k_0 h_m)\right] \qquad E_m \neq \pm k_0$$

$$\text{(eqn 3.39)}$$

$$N_{\theta m} = N_{\theta_0} h_m \sin(k_0 h_m) \qquad\qquad E_m = \pm k_0$$

$$\text{(eqn 3.40)}$$

and

$$N_{\varphi m} = N_{\varphi 0} \frac{-2k_0}{E_m^2 - k_0^2} \left[\cos(E_m h_m) - \cos(k_0 h_m) \right] \qquad E_m \neq \pm k_0$$

(eqn 3.41)

$$N_{\varphi m} = N_{\varphi 0} \, h_m \sin(E_m h_m) \qquad E_m = \pm k_0$$

(eqn 3.42)

where

$$N_{\theta 0} = \frac{\sin\psi_m \cos\theta \sin\varphi - \cos\psi_m \sin\theta}{\sin(k_0 h_m)} I_m \, e^{j[k_0(y_m \sin\theta \sin\varphi + z_m \cos\theta)]}$$

(eqn 3.43)

$$N_{\varphi 0} = \frac{\sin\psi_m \cos\varphi}{\sin(k_0 h_m)} I_m \, e^{j[k_0(y_m \sin\theta \sin\varphi + z_m \cos\theta)]}$$

(eqn 3.44)

$$E_m = k_0(\sin\psi_m \sin\theta \sin\varphi + \cos\psi_m \cos\theta)$$

(eqn 3.45)

In this thesis, only the monostatic radar cross section will be considered. In the radiation equations the angles θ and φ represent the orientation angles of the scattered electric field $\hat{E}^S$. Their relation with the incident angles θ_0 and φ_0 for the monostatic case is:

$$\theta = \pi - \theta_0$$

(eqn 3.46)

$$\varphi = \pi - \varphi_0$$

(eqn 3.47)

If M denotes the total number of PWS modes in the structure under investigation, then

$$N_\theta = \sum_{m=1}^{M} N_{\theta m}$$

(eqn 3.48)

$$N_\varphi = \sum_{m=1}^{M} N_{\varphi m}$$

(eqn 3.49)

25

The final expression for the equations 3.24 and 3.25 is

$$E_\theta = C \cdot \sum_{m=1}^{M} N_{\theta m} \qquad \text{(eqn 3.50)}$$

$$E_\varphi = C \sum_{m=1}^{M} N_{\varphi m} \qquad \text{(eqn 3.51)}$$

where

$$C = \frac{-jk_0 e^{-jk_0 r}}{4\pi r} \eta \qquad \text{(eqn 3.52)}$$

3.   RCS Equations

When an incident plane wave with electric field $\hat{E}^i$ strikes the object and $\hat{E}^S$ is the scattered electric field, the radar cross section σ is defined as

$$\sigma = \lim_{r \to \infty} 4\pi r^2 \frac{|\hat{E}^S|^2}{|\hat{E}^i|^2} \qquad \text{(eqn 3.53)}$$

For the scattered electric field $\hat{E}^S$, its spherical coordinates E_θ, and E_φ have been calculated by the equations 3.50 and 3.51. The incident electric field $\hat{E}^i$ is known by means of equation 3.11.

$$|\hat{E}^i|^2 = |a|^2 + |b|^2 + \left| \frac{ak_y + bk_z}{k_x} \right|^2 \qquad \text{(eqn 3.54)}$$

$$|\hat{E}^S|^2 = |E_\theta|^2 + |E_\varphi|^2 = |C|^2 \left[[|N_\theta|^2 + |N_\varphi|^2 \right]$$

$$\text{(eqn 3.55)}$$

26

The combination of equations 3.11, 3.50–3.52, 3.54–3.55, and 3.53 leads to the final formula for RCS:

$$\sigma = \frac{k_0 \eta^2}{4\pi} \left[|N_\theta|^2 + |N_\varphi|^2 \right] \frac{1}{|a|^2 + |b|^2 + \left| \dfrac{ak_y + bk_z}{k_x} \right|^2}$$

(eqn 3.56)

This is the formula that the program uses to compute the RCS of a planar structure for a given set of incident angles θ_0, and φ_0.

B. INPUT–OUTPUT OF RCS PROGRAM

The RCS program, which is described in Appendix A, is a FORTRAN program having two input files. The first input file, *INPUT1*, contains the data that characterize the incident plane wave and the data that describe the geometry of the planar structure whose broadside RCS is measured. The second input file, *INPUT*, contains the set of incident angles θ_0, φ_0.

The program reads from the INPUT1 file the following input data:

1. frequency of the incident plane wave in GHz,

2. parameters a and b that characterize the polarization of the incident electric field.

3. number of dipoles that the structure consists of,

4. half length of each dipole in cm,

5. half width of each dipole in cm,

6. coordinates in cm of the center of each dipole along the two axes of the orthogonal system that the structure lies,

27

7. orientation angle of each dipole, measured from the vertical axis, positive in the clockwise direction, and

8. number of segments of each dipole.

As the program reads these input data it generates the geometry of the PWS modes, calculates the impedance elements between any two modes of the structure, and fills the impedance matrix [Z]. The size of the impedance matrix depends on the total number of modes. When this matrix is calculated and filled, the program inverts it to $[Z]^{-1}$ and stores it for later use.

The next step is to read from the *INPUT* file the sets of incident angles θ_0, φ_0 and for each one it calculates the voltage on each mode, filling the voltage matrix [V]. This matrix is a column vector which depends upon the excitation only. Then it multiplies the stored inverted impedance matrix $[Z]^{-1}$ by the voltage matrix. This yields the current vector [I]:

$$[I] = [Z]^{-1} \cdot [V] \qquad \text{(eqn 3.57)}$$

As the induced currents are known, the program uses the previously described radiation equations and calculates the RCS of the structure corresponding to the given set of incident angles θ_0, φ_0. The output RCS is normalized to the square of the wavelength λ^2, and is given in dB. The program reads the next set of incident angles θ_0, φ_0 and repeats the same procedure to compute the RCS of the new set.

Although the input lengths and widths are in cm, the program considers them normalized to the wavelength. For accurate results at least 4 segments per wavelength are chosen. The selection of the width of each dipole is arbitrarily taken as L/W = 33.

IV. FRACTAL TREE GENERATION

The problem of measuring the radar cross section of a real natural tree is complicated as it requires an investigation in three dimensional space with very long, intersecting elongated objects that are randomly oriented.

For simplicity the radar cross section (RCS) problem is solved in a two dimensional space. RCS is calculated from a planar fractal tree whose branches are considered as thin planar dipoles of different lengths and widths. In an actual tree, the branches are lossy and in general anisotropic. However, in the present model, the tree is comprised of perfectly conducting branches. The geometry of this tree is based upon the fractal geometry.

A. DEFINITIONS

Fractal is a mathematical set or object whose form is extremely irregular or fragmented at all scales [Ref. 6]. The requirement to describe the shape of many objects that appear in the natural world, such as trees, mountains, coastlines, etc., led to the generation of fractal geometry. As Euclidean geometry cannot give mathematical expressions to describe fractal objects, fractal geometry is used to describe mathematically many natural patterns.

The basic characteristics of fractal objects are [Ref. 7]:

1. A large degree of heterogeneity.

2. A self–similar structure over many size scales. Self–similarity refers to the general preservation of form or characteristic regardless of the scale of observation.

3. The lack of a well–defined (characteristic) scale.

The geometric characteristics of fractal objects are useful for describing phenomena of nature, such as scattering of objects like landscapes or surface cracks. Although these objects are irregular and randomly oriented in nature, they show structural similarities on several different discrete size scales [Ref. 7].

One measure of structural complexity is the fractal dimension D_F. There are several definitions of D_F depending upon the particular application. For the case of fractal trees the fractal dimension D_F is the measure of the space that a self–similar structure fills, and it varies with the branching levels that the structure consists of.

The most useful terms from fractal geometry that are used to describe a planar fractal tree are the following:

1. The number of branch segments N formed from each preceding branch segment.

2. The constant similarity ratio "r" that relates the fractional reduction in segment length for each segment to previous level. this factor is less than 1.0.

In this case, the fractal dimension D_F is given by the formula [Ref. 7]:

$$1 - D_F = \frac{\log(\text{total branch length})}{\log(\text{average branch length})} = \frac{\log(rN)}{\log(1/r)}$$

This equation is accurate for symmetric structures or asymmetric structures having a normal distribution function [Ref. 7]. More details about fractal geometry are discussed in [Ref. 1] and [Ref. 7].

B.   FRACTAL TREE GENERATION

In the planar fractal structures that are used for calculating the radar cross section, the number of branch segments N formed from each preceding branch segment is 2. The principal properties of these trees are that the branches are not overlapping, and the angle θ between any two branches is the same. The nonoverlapping between the branches of each fractal model is achieved by choosing the branch angle θ for a given reduction factor by the following empirical formula [Ref. 7]

$$\text{Minimum } \theta = 32.34 \times r^{6.77} \qquad \text{(Radians)}$$

This angle is given in radians and r is the desired reduction factor which is a constant for the structure. As the reduction factor r increases the tree fills more space.

Five types of planar fractal trees are considered in this thesis. Each type corresponds to a set of values for reduction factor r and minimum branch angle θ. Table 4.1 shows these sets of r and minimum θ, where θ is given in degrees.

Each model is generated by selecting the desirable reduction factor r (r < 1.0), the corresponding branch angle θ given by equation 4.1, the initial length from which the reduction will start, the value of N (which in the investigated case is 2),

and the number of the desired levels for branch generation. Each level contains 2^r points corresponding to the end points of the reduced length branches.

TABLE 4.1

NUMERICAL VALUES OF r AND MINIMUM ANGLE θ.

REDUCTION FACTOR (r)	ANGLE θ
0.53	29.94^0
0.55	46.43^0
0.60	95.89^0
0.66	145.35^0
0.71	180.00^0

Figures 4.1–4.5 show the planar fractal trees that correspond to each set of r and θ of Table 4.1 respectively. As the branch angle θ increases, the spreading of the branches becomes larger. In all trees the physical length of the initial branch is chosen as two centimeters. These models were generated by a FORTRAN program which has the following input data:

1. The initial length. This the length of the first dipole whose length will be reduced by the constant reduction factor (r).

2. The value of N, being 2 in all cases.

3. The initial point that the reduction starts. This point is the end point of the initial wire.

4.   The number of desirable levels for branch generation.

5.   The branch angle θ.

The program generates two output files. The first is the input file for the RCS program containing all the required data that were mentioned in Chapter 3. The second output file contains the coordinates of the start and end points of each generated branch.

For the models characterized by reduction factors 0.53, 0.55, and 0.60, the program limits the structure size when the length of a branch becomes smaller than 0.1 of the wavelength of the incident plane wave. For the models characterized by reduction factor 0.66 and 0.71, this limit is taken as 0.15. The reason is that as the reduction factor increases the number of branches in a particular branch level increases. The size of the tree is truncated so that the number of unknowns is manageable.

The geometry of all planar fractal trees is in the same coordinate system that the RCS program uses. All models have been generated in the y–z plane of a cartesian coordinate system.
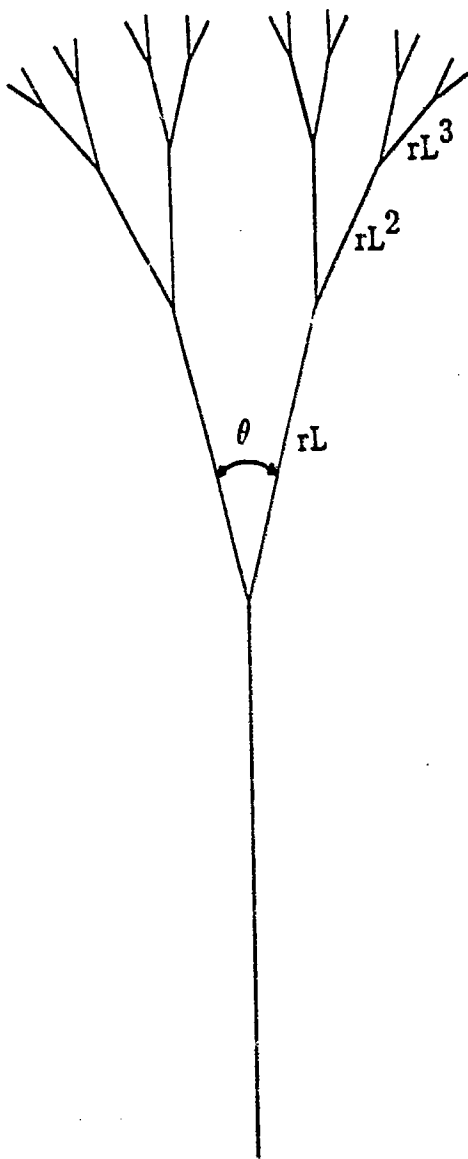
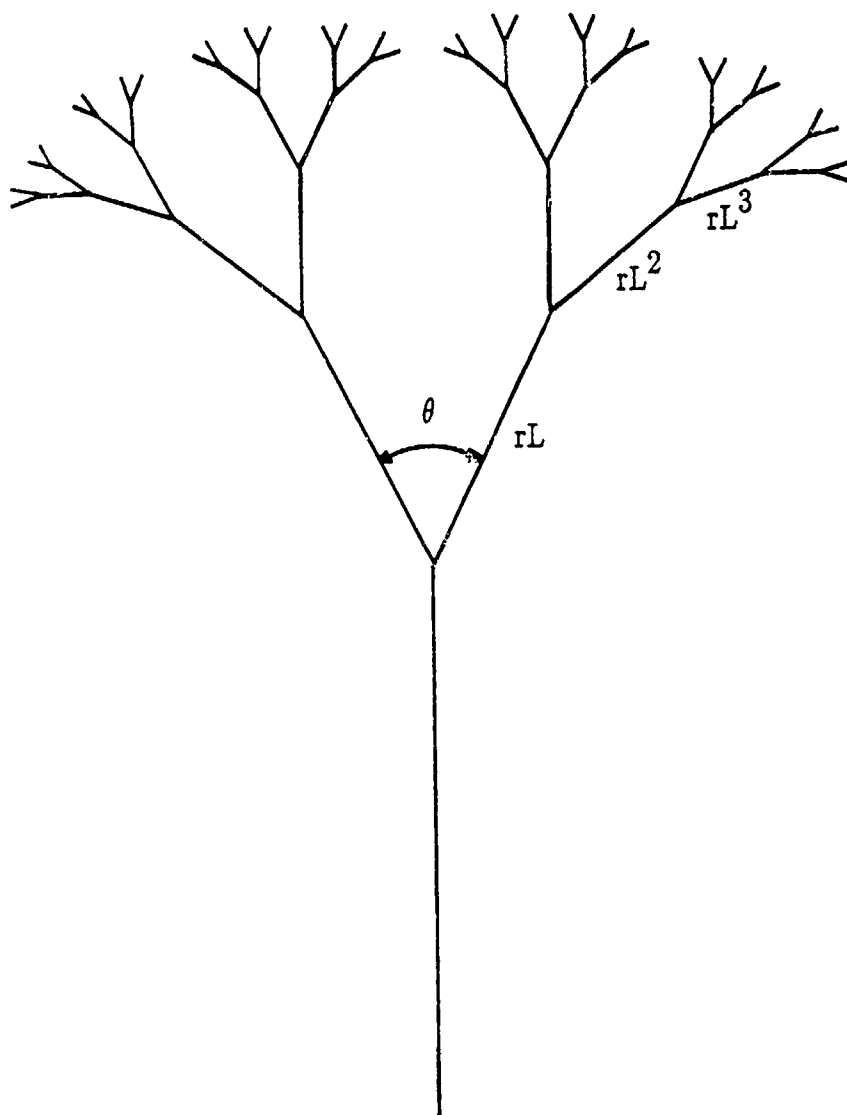Figure 4.1 Fractal Tree for r = 0.53 and $\theta = 29.94^\circ$.

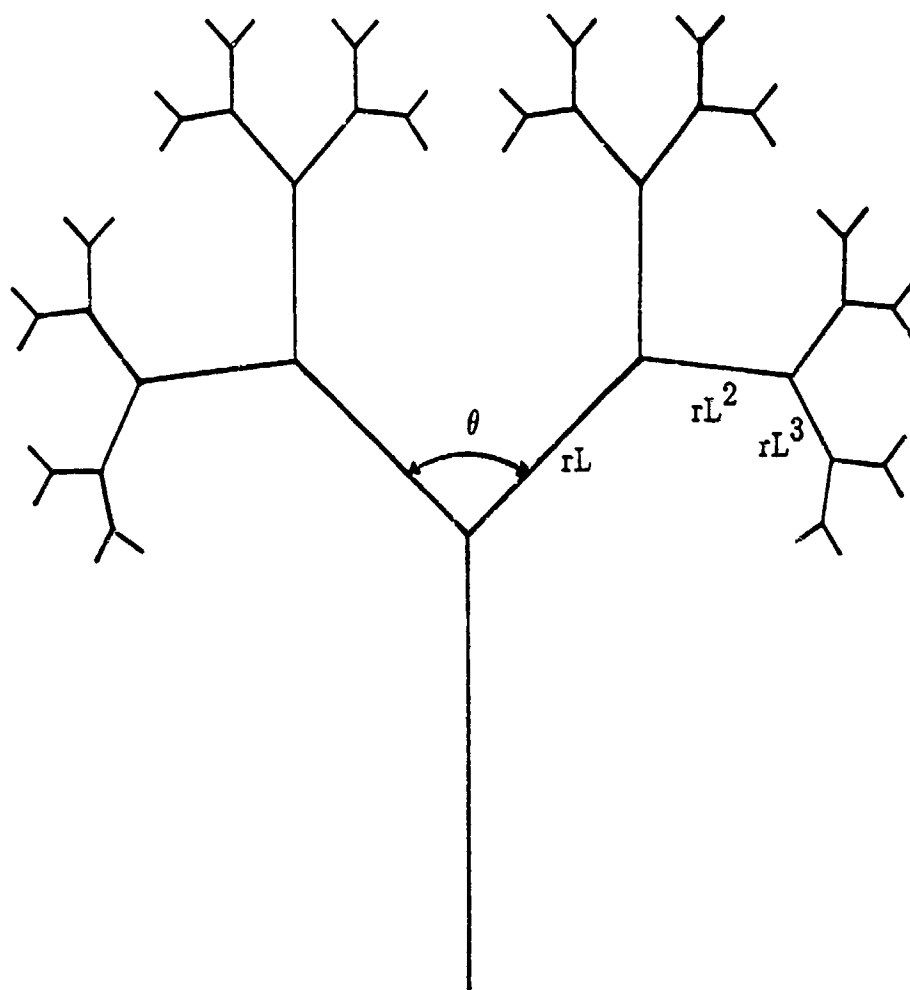Figure 4.2 Fractal Tree for r = 0.55 and $\theta = 46.43^0$.

Figure 4.3 Fractal Tree for $r = 0.60$ and $\theta = 95.89^{\circ}$.
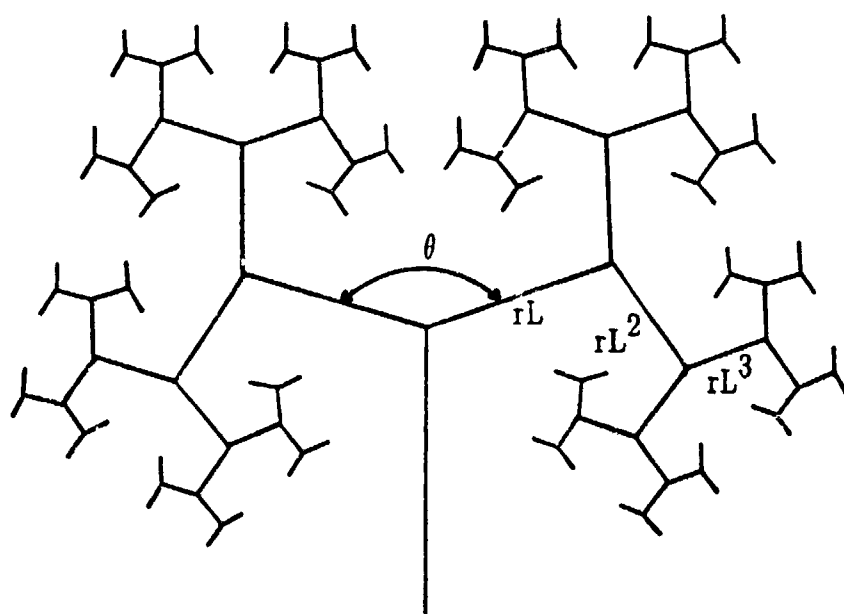
Figure 4.4   Fractal Tree for $r = 0.66$ and $\theta = 145.35^0$.
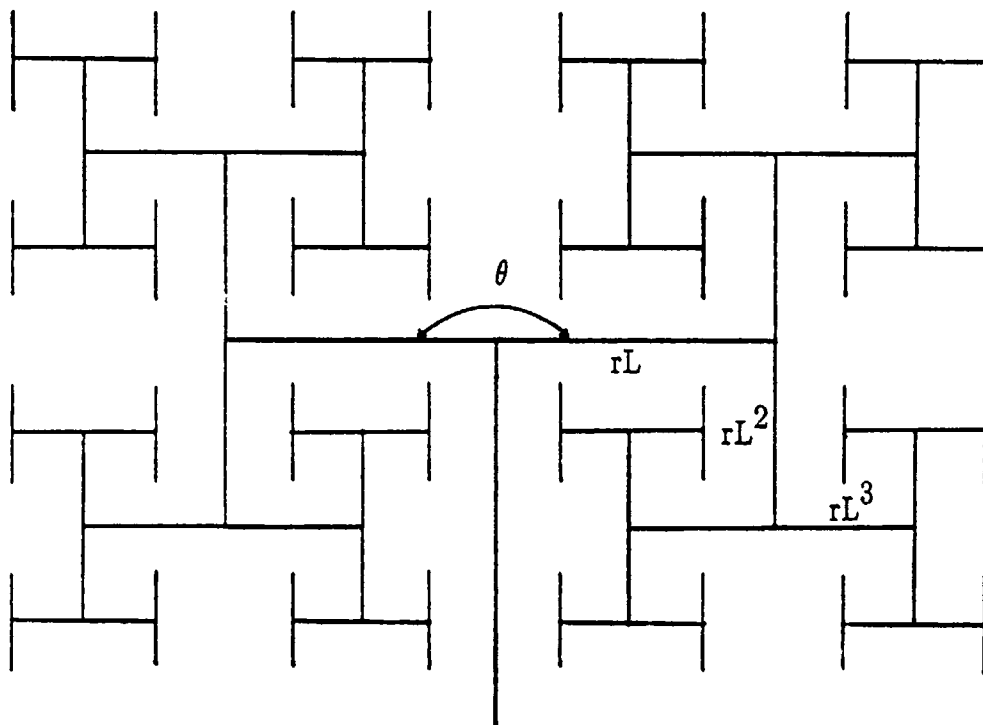
Figure 4.5 Fractal Tree for r = 0.71 and $\theta = 180^0$.

V. NUMERICAL RESULTS

In this chapter, computed results for the radar cross section σ of planar structures are presented. In order to check the program, the radar cross section results of a single planar dipole are compared with the results given in [Ref. 8]. Details of this comparison are presented in the following section.

In all models where numerical results for the radar cross section are presented, the following factors have been considered:

1. E–plane is the plane corresponding to $\varphi_0 = 0^0$, and θ_0 varying from 0^0 to 180^0.

2. H–plane is the plane corresponding to $\theta_0 = 90^0$, and φ_0 varying from -90^0 to $+90^0$.

3. The resulting RCS σ is normalized to the square of the wavelength λ of the incident plane wave (σ/λ^2).

4. The number of segments, that each dipole is subdivided, is taken as four per wavelength.

5. The physical dimensions and orientations of the dipoles used to construct a planar structure are the same when this structure is investigated at different frequencies, and only the segmentation is different depending upon the wavelength λ of the incident plane wave.

6. Each PWS mode has length equal to the length of two segments.

7. The incident electric field is linearly polarized and the parameters a and b are taken as 0 and 1 respectively for this investigation. This corresponds to having only a horizontal magnetic field.

A.   SCATTERING FROM A SINGLE DIPOLE

In Figure 5.1 a centered loaded vertical planar thin dipole of length L and width 2w is oriented along the z axis. This dipole is excited by a plane wave of frequency 30 GHz traveling in the x–y plane ($\theta_0 = 90^0$, $\varphi_0 = 0^0$). The same situation is described in [Ref. 8, pp. 510–515] for a cylindrical dipole of radius a and length L such that L/2a=74.2. In the present case of a planar dipole, the length of the planar dipole is selected such that L/2w = 33 [Ref. 9]. Figure 5.2 shows, on a semi–log scale, the results computed by the developed program of the monostatic normalized radar cross section σ/λ^2 of this single dipole for values of L/λ ranging from 0 to 1.4, and for loads $Z_L = 0$ and $Z_L = \infty$. The case of $Z_L = \infty$ is achieved by setting a small gap (0.01 wavelength) at the center of this planar dipole. In Figure 5.2, the corresponding values of σ/λ^2 from [Ref. 8, pp. 115] are also shown.

This comparison leads to an accurate check of the correct calculation of the radar cross section by the developed RCS program. The small discrepancy between the computed values and those given by [Ref. 8] is due to the error incurred in reading values off the curves presented in [Ref. 8, pp. 115].
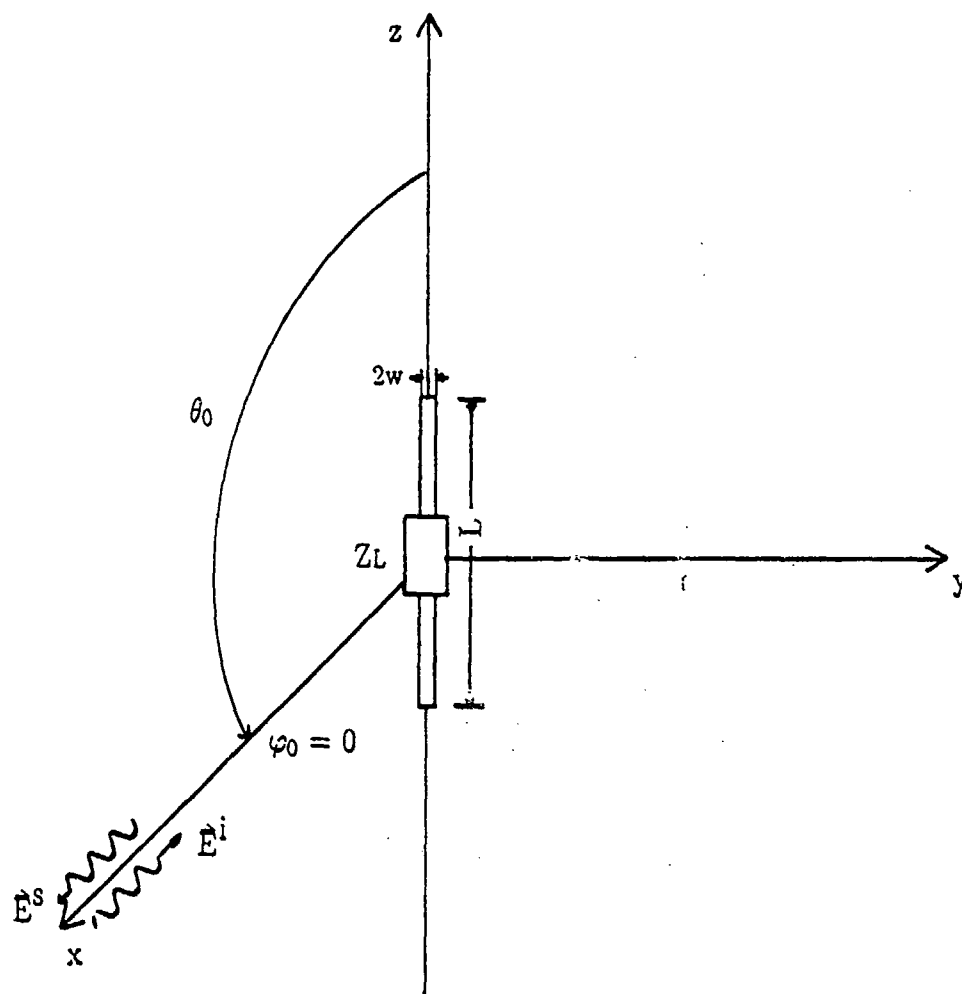
Figure 5.1 Vertical Centered Loaded Planar Dipole.
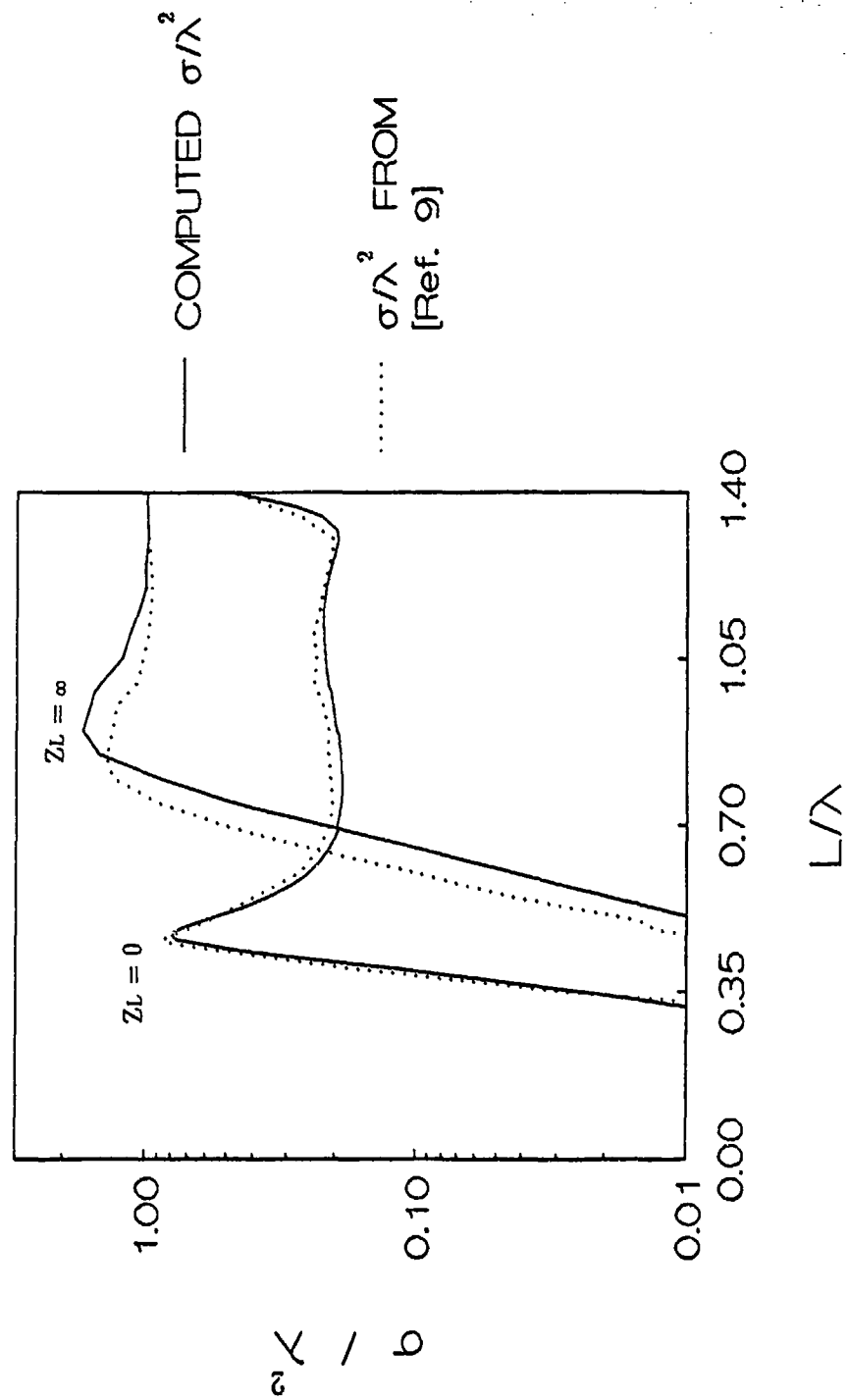
Figure 5.2 Normalized RCS σ/λ^2 of a Center Loaded Planar Dipole.

B. SCATTERING FROM PLANAR FRACTAL TREES

In Chapter 4, five types of planar fractal trees were described. Each type of these trees was lying in the y–z plane. The developed RCS program calculates the broadside radar cross section σ of each tree for frequencies 15 GHz–75 GHz, for the monostatic case. The initial dipole that is being reduced by the reduction factor r has physical length 2 cm and only the branch lengths are changed for each tree depending upon the reduction factor r. As the frequency of the plane wave changes, the electrical length of this dipole as well as the dipoles composing the tree will also change. For the frequency range of 15 GHz–75 GHz, the electrical length of the initial length will vary from one to four wavelengths.

Figures 5.3–5.6 show the variations of σ/λ^2, in dB, in the E–plane and the H–plane for the case of a fractal tree characterized by reduction factor r = 0.53 and branch angle θ = 29.94^0. The frequency of the incident plane wave varied from 15 GHz to 60 GHz in steps of 15 GHz. The tree is composed of 31 dipoles. This number is small as the reduction factor is small and the branch lengths are reduced to very small values at low levels.

The σ/λ^2 variations in the E–Plane are in a range of 10 dB approximately. In the H–Plane. The σ/λ^2 is symmetric about the 90^0 axis and is smoother at lower frequencies. As the frequency increases, the maximum value of σ/λ^2 at θ_0 = 90^0 and φ_0=0^0, increases from 2.73 dB at 15 GHz to 19.23 dB at 60 GHz. Figure 5.7 shows the variation of the maximum σ/λ^2 in terms of frequency increments for the same structure. This variation is very small between 30 and 45 GHz.

Figure 5.3 Normalized RCS in dB at F = 15 GHz of a Fractal Tree

with r = 0.53 and θ = 29.94⁰.

Figure 5.4 Normalized RCS at F = 30 GHz of a Fractal Tree

with r = 0.53 and θ = 29.94°.

Figure 5.5 Normalized RCS at F = 45 GHz of a Fractal Tree
with r = 0.53 and θ = 29.94⁰.

Figure 5.6 Normalized RCS at F = 60 GHz of a Planar Fractal Tree

with r = 0.53 and θ = 29.94°.

Figure 5.7 Variation of maximum σ/λ^2 vs. Frequency
of a Planar Fractal Tree with r = 0.53 and θ =29.94⁰.

Figures 5.8–5.12 show the variations of σ/λ^2, in dB, in the E and H planes for the fractal tree characterized by a reduction factor r = 0.55 and branch angle θ = 46.43⁰. In this case, the fractal tree is composed of 63 dipoles and spreads more than the previous one, and the lengths of the branches are bigger than the previous ones (due to a larger reduction factor of 0.55 instead of 0.53). This results in more variations for σ/λ^2 in both E and H planes.

This model is investigated at a frequency range of 15–75 GHz. At all frequencies, the σ/λ^2 varies in a range of 10–12 dB approximately. In the H–Plane the variation of σ/λ^2 is symmetric about the 90⁰ axis. The maximum value of radar cross section varies from 2.78 db at 15 GHz to 22.63 dB at 75 GHz. Figure 5.13 shows the maximum value of σ/λ^2, corresponding to θ_0 = 90⁰ and φ_0 = 0⁰ in terms of the frequency of the incident plane wave, varying from 15 GHz to 75 GHz. This maximum σ/λ^2 increases linearly as the frequency increases except the range of 45–60 GHz where the variation is very small.

Figure 5.8 Normalized RCS at F = 15 GHz of a Planar Fractal

with r = 0.55 and θ = 46.43^0.

Figure 5.9 Normalized RCS at F = 30 GHz of a Planar Fractal Tree
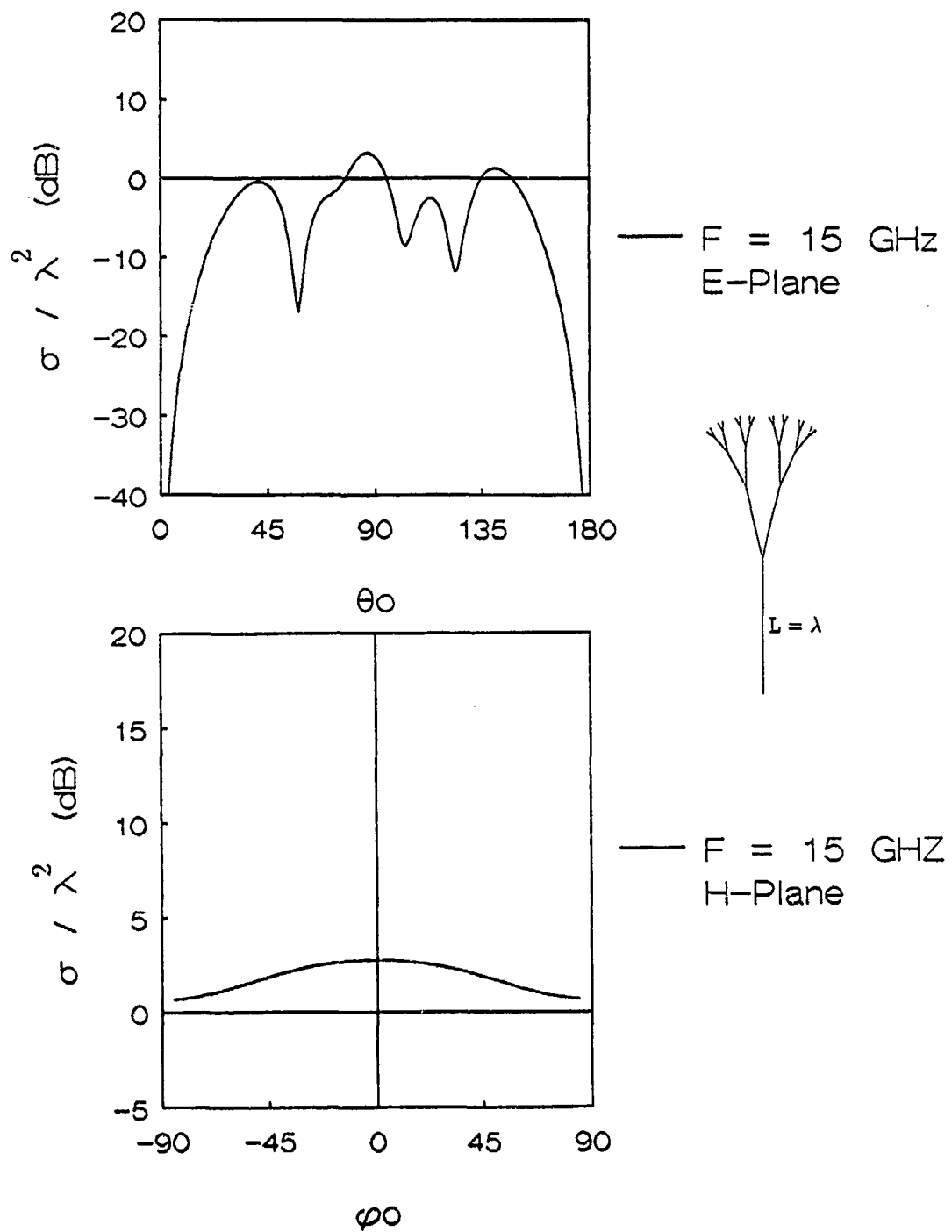
with r = 0.55 and $\theta = 46.43^0$.

Figure 5.10 Normalized RCS at F = 45 GHz of a Planar Fractal Tree
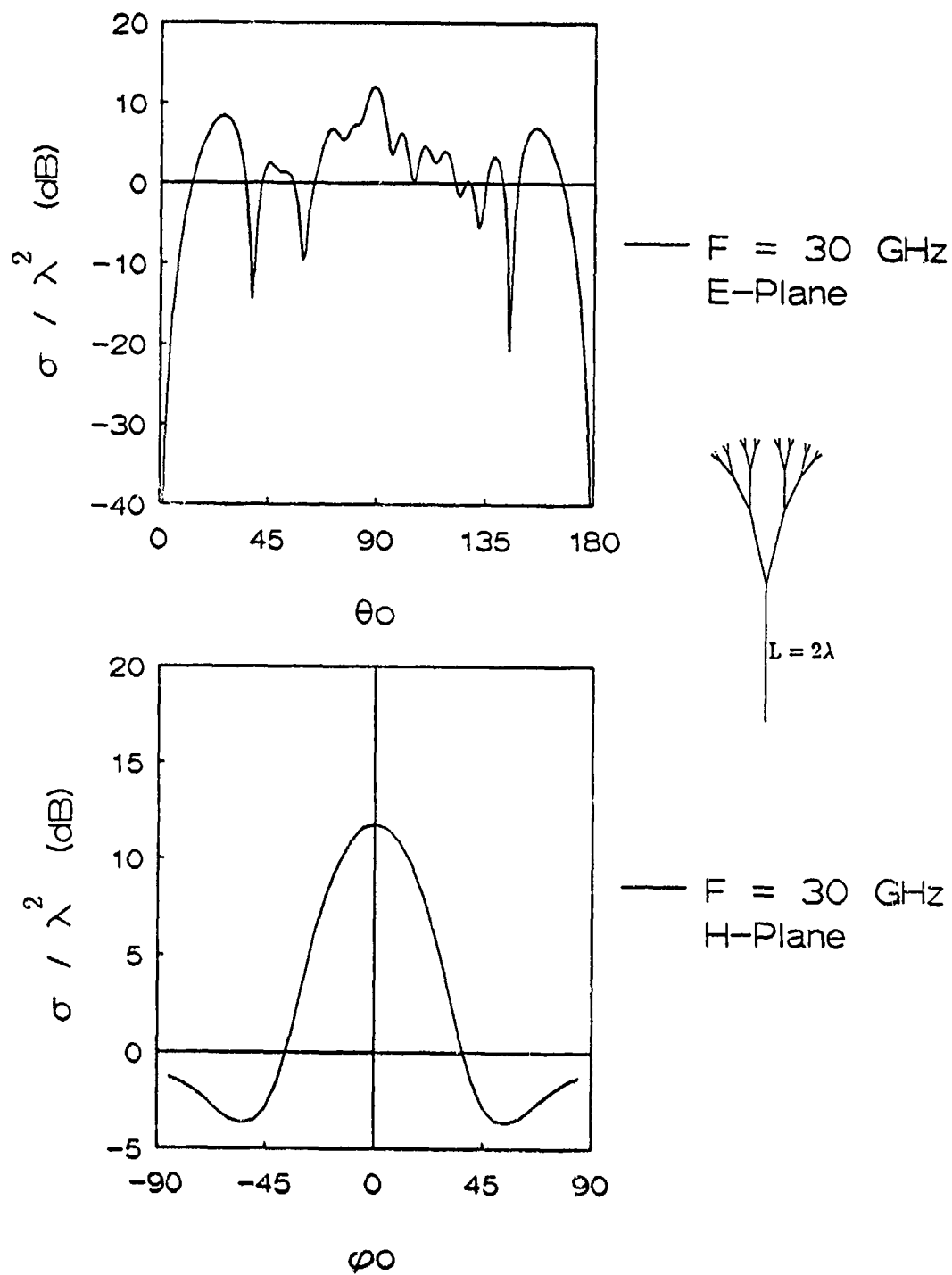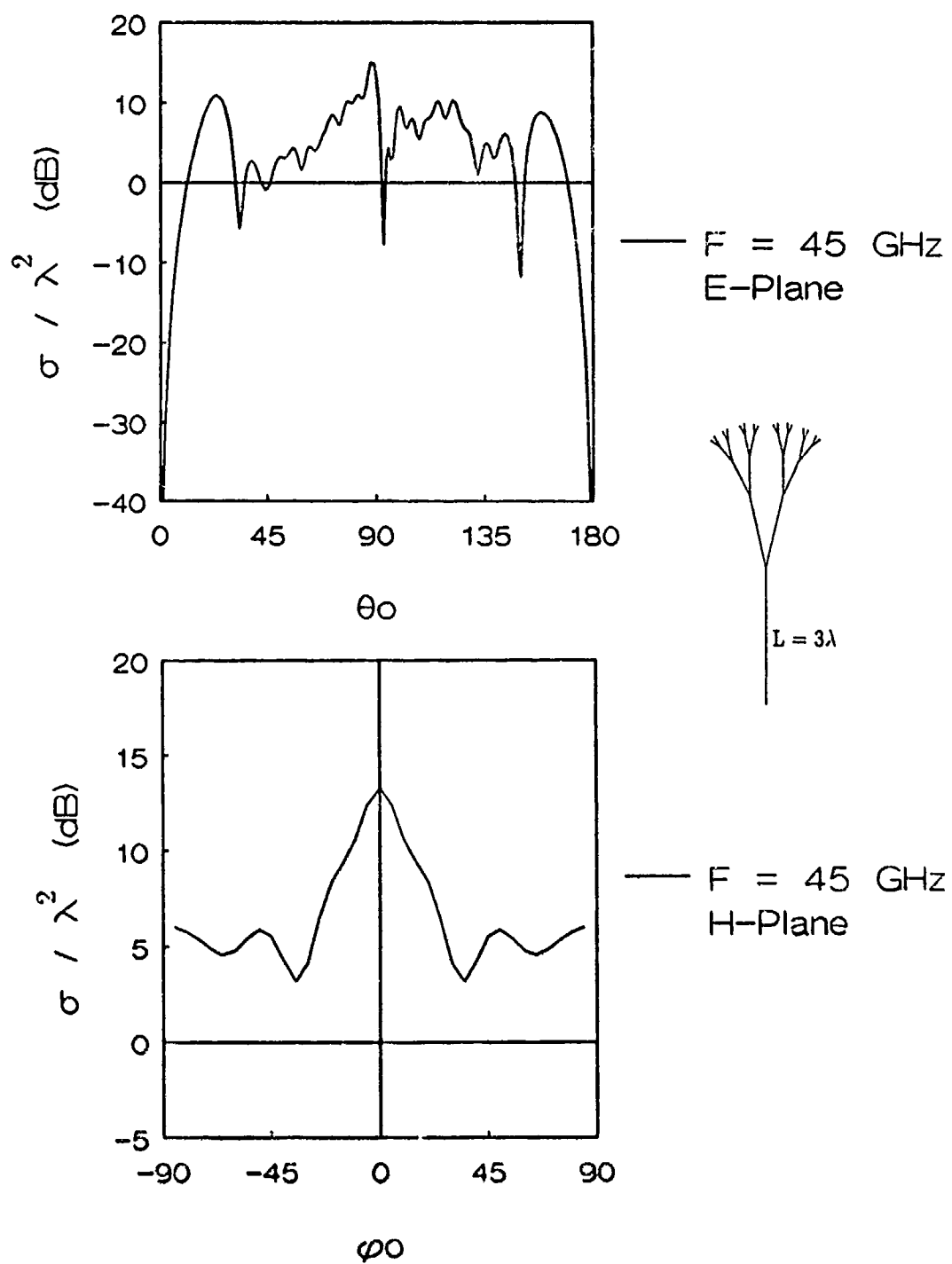with r = 0.55 and $\theta = 46.43^0$.

Figure 5.11 Normalized RCS at F = 60 GHz of a Planar Fractal Tree
with r = 0.55 and θ = 46.43°.
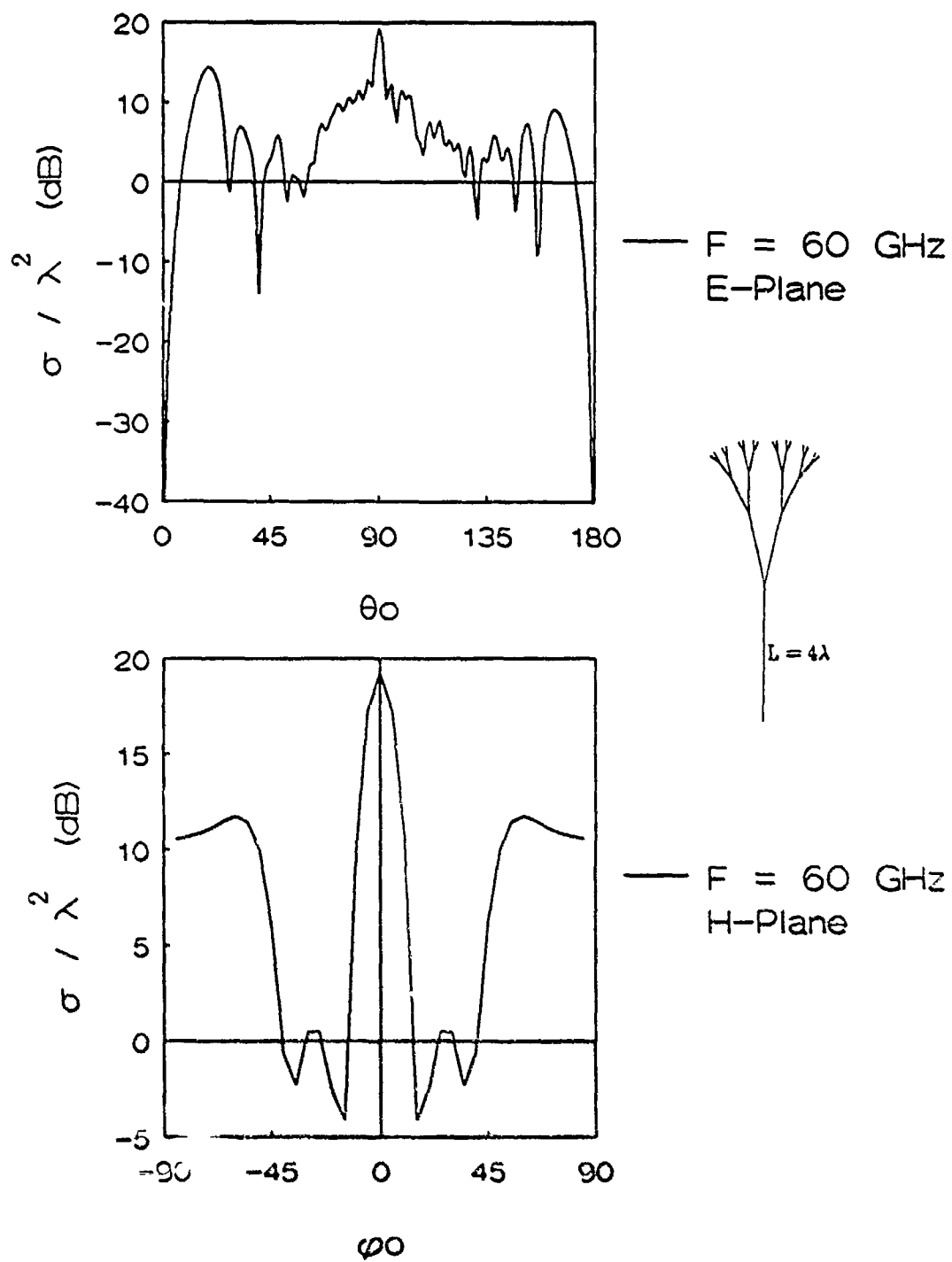
Figure 5.12 Normalized RCS at F = 75 GHz of a Planar Fractal Tree
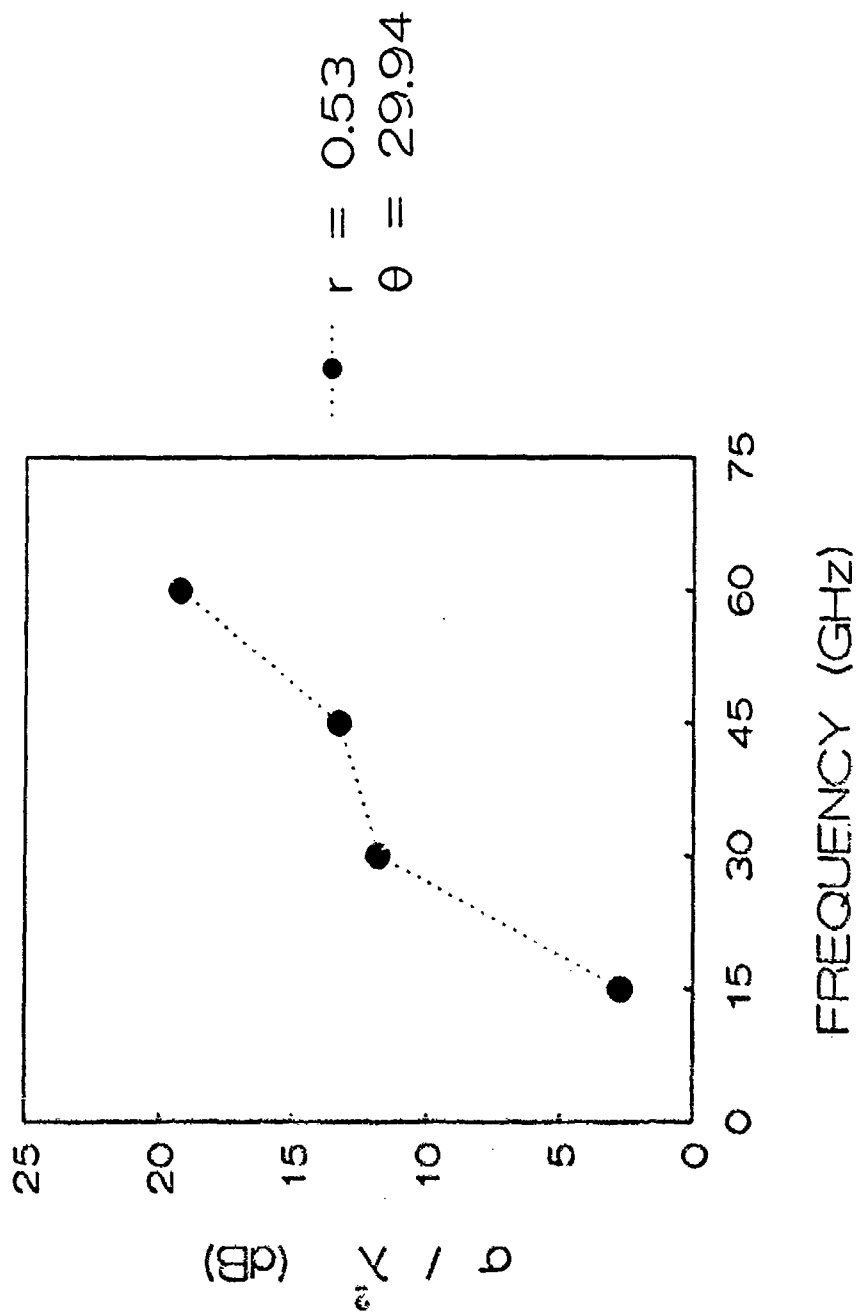with r = 0.55 and $\theta = 46.43^0$.
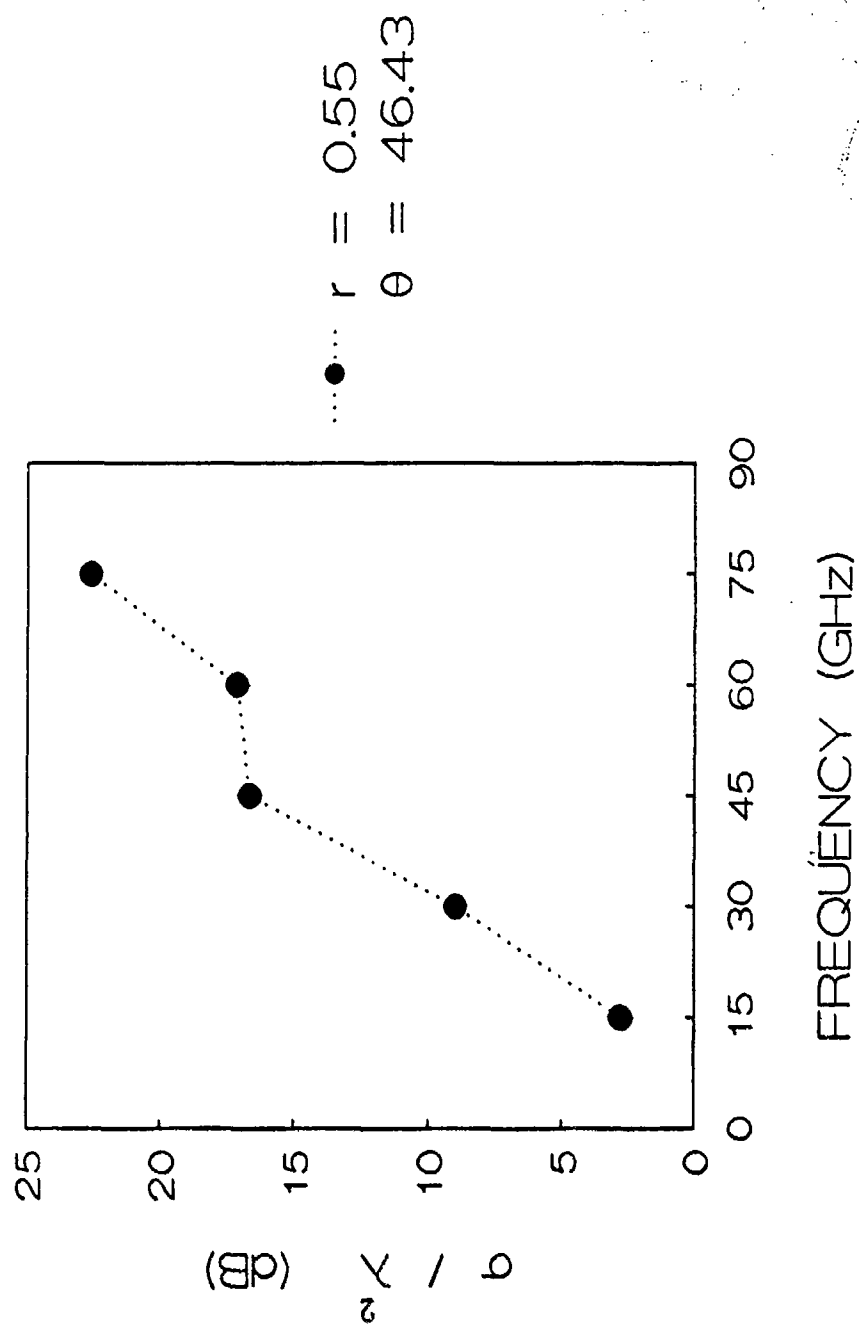
Figure 5.13 Variation of Maximum RCS vs. Frequency

of a Planar Fractal Tree with r = 0.55 and θ = 46.43⁰.

Figures 5.14–5.18 show the variations of the normalized radar cross section σ/λ^2 of a planar fractal tree characterized by reduction factor r = 0.60 and branch angle θ = 95.89⁰. This model is composed of 63 dipoles and has more spreading than the two models that were previously investigated. The branches have larger physical lengths than the ones in other two models. At 15 GHz, the variation of σ/λ^2 in the E–Plane is very low and similar to the variation in the other two models at the same frequency. In the H–Plane this variation is different as the incident plane wave strikes more dipoles from –90⁰ to 90⁰.

As the frequency increases, the electrical length of the dipoles is also increased, and more lobes appear at 30 GHz and higher frequencies in both the E and the H planes. The maximum value of σ/λ^2 at θ_0= 90⁰ and φ_0 = 0⁰ varies from –0.23 dB at 15 GHz to 21.60 dB at 75 GHz. Figure 5.19 shows the variation of the maximum radar cross section in terms of the frequency of the incident plane wave. In a range of 15–60 GHz the values of maximum σ/λ^2 follow a straight line approximately. In the range of 60–75 GHz the variation of maximum σ/λ^2 is small.

The planar fractal trees characterized by r = 0.66, θ = 145.35⁰, and r = 0.71, θ = 180⁰, have large values of branching angles. The large values of reduction factor r generate fractal trees whose branches have large physical lengths compared with the lengths of the branches of the previously investigated fractal trees. The result is that the electrical lengths of these branches are large also at the range of 15–75 GHz, and a large number of modes is required to investigate the last two types of fractal trees. It was found that the developed RCS program is not able to calculate the radar cross section of fractal trees that are characterized by large values of reduction factor r and branching angle θ due to memory restrictions and other numerical problems.

For this reason the numerical results for σ/λ^2 are not presented in this thesis for these two cases.

It is seen by comparing Figures 5.7, 5.13, and 5.19 that there is a frequency range over which the variation of maximum RCS is rather small. Furthermore, this range of frequencies shifts to higher frequencies as the tree structure is spread from r = 0.53 to r = 0.60. The maximum RCS of each of these trees varies in a range of 3 dB approximately at the same frequency.

Scattering from an actual tree will not exactly follow all these patterns, but it is felt that the trends would generally remain the same. This is specially true for the frequency behavior.
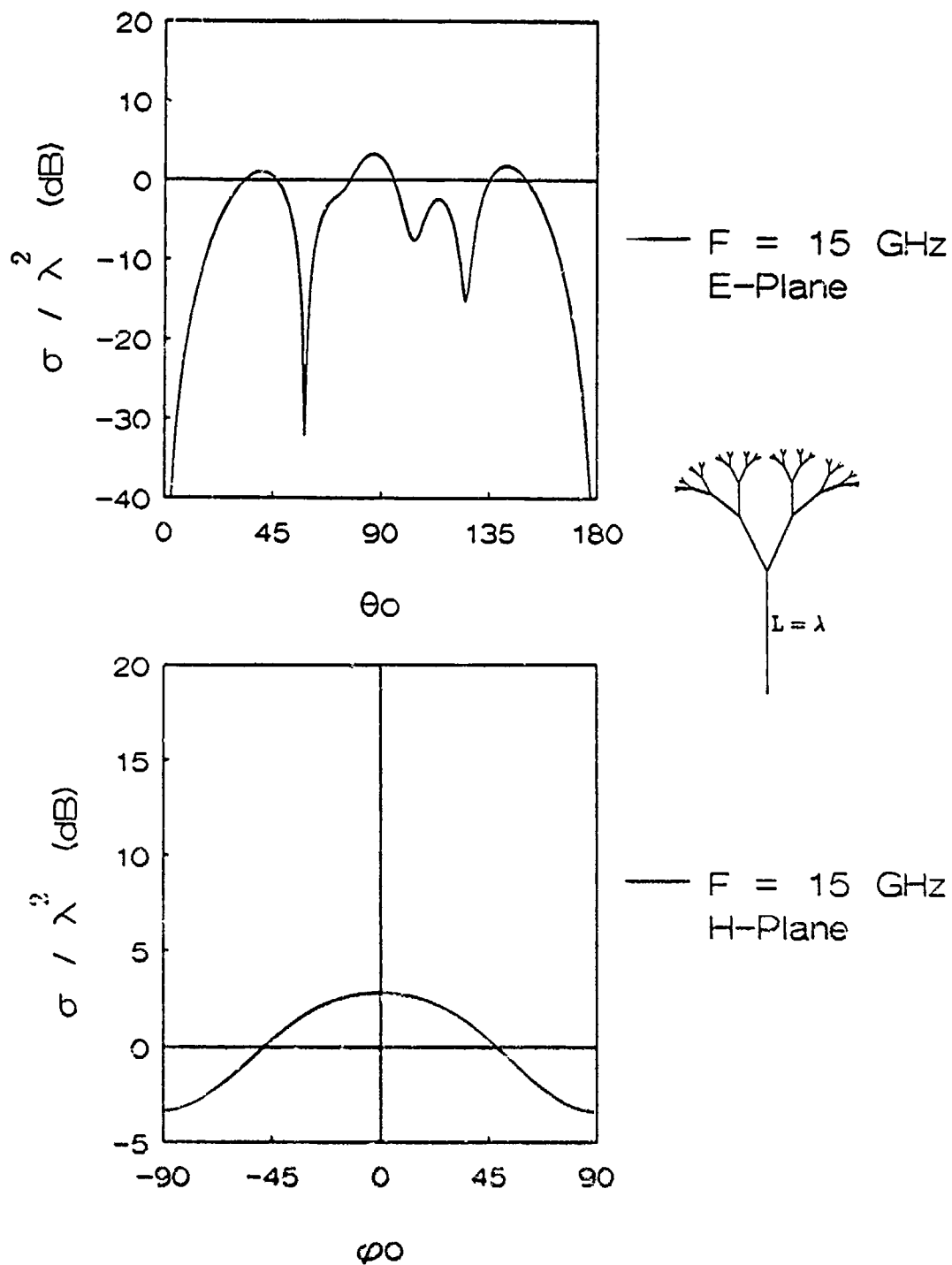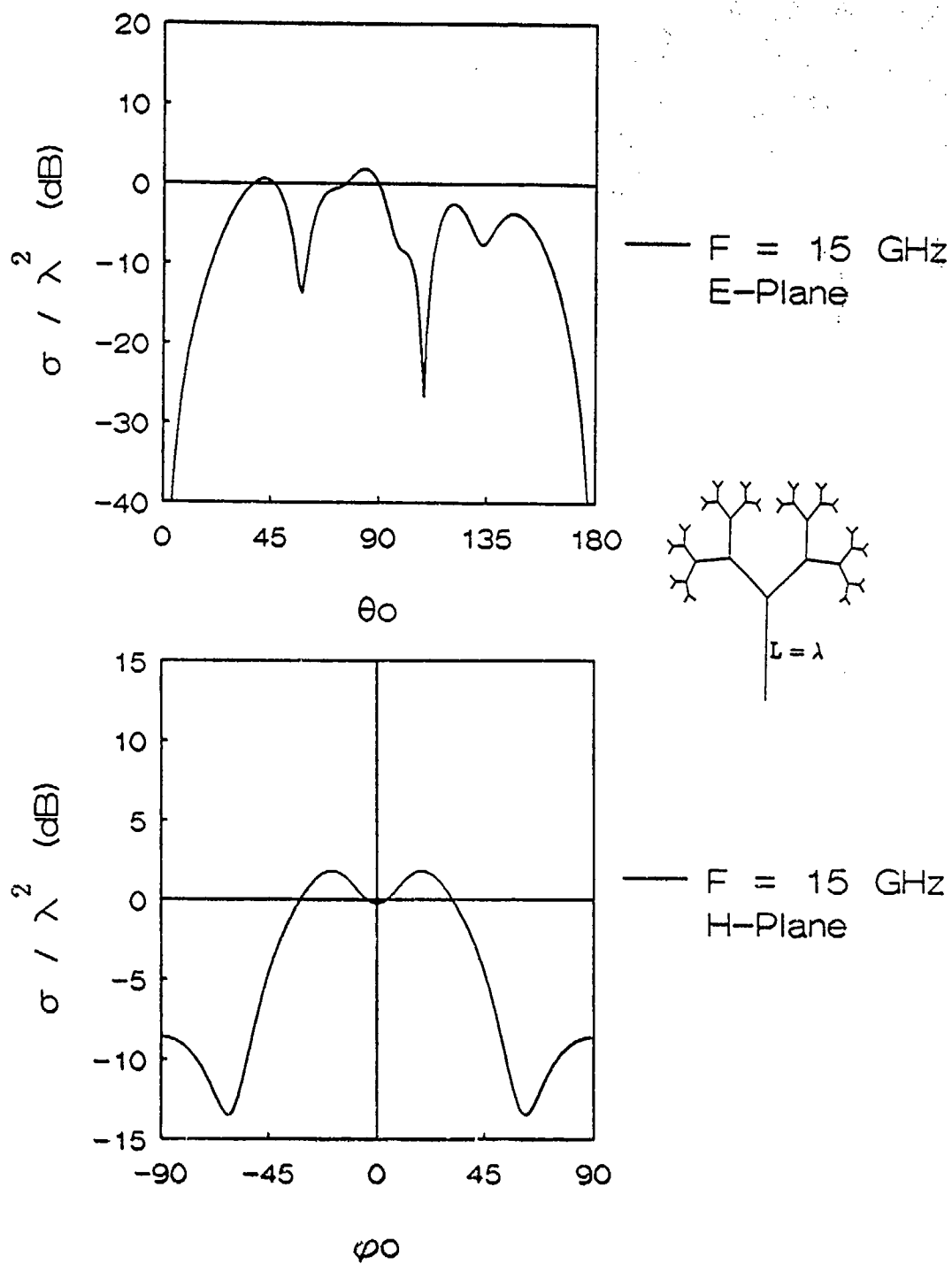
Figure 5.14 Normalized RCS at F = 15 GHz of a Planar Fractal Tree
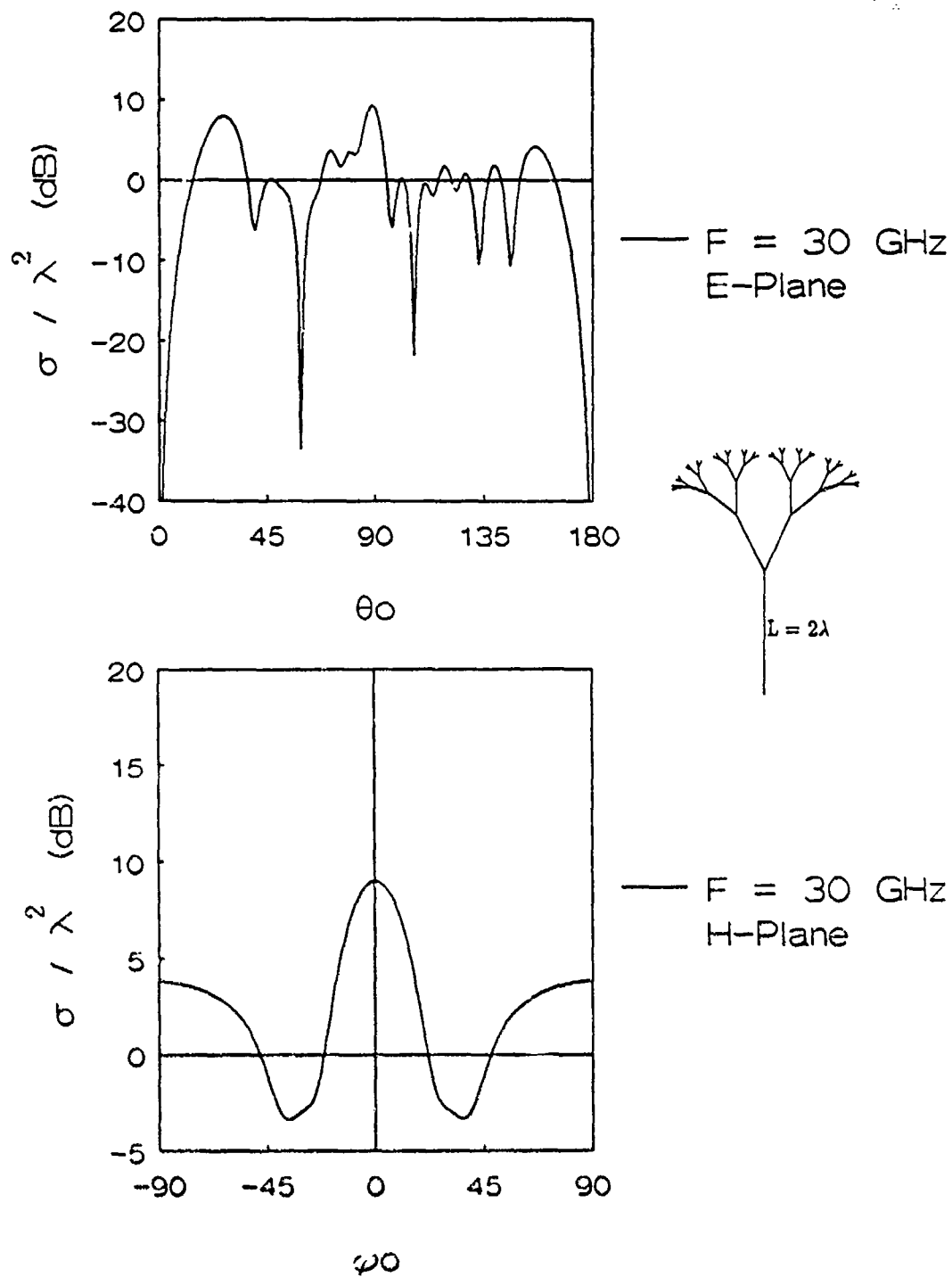with r = 0.60 and θ = 95.89º.
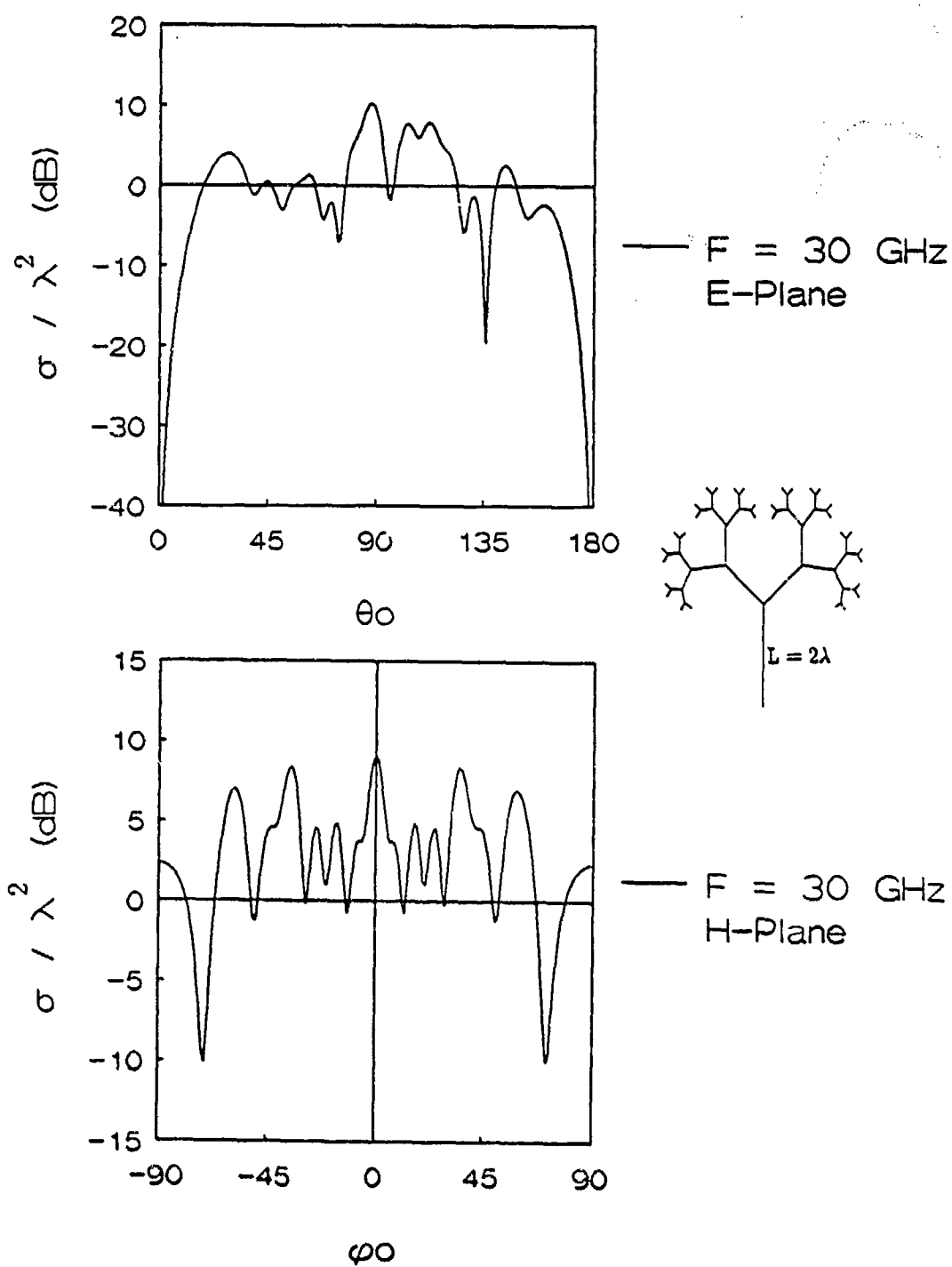
Figure 5.15 Normalized RCS at F = 30 GHz of a Planar Fractal Tree
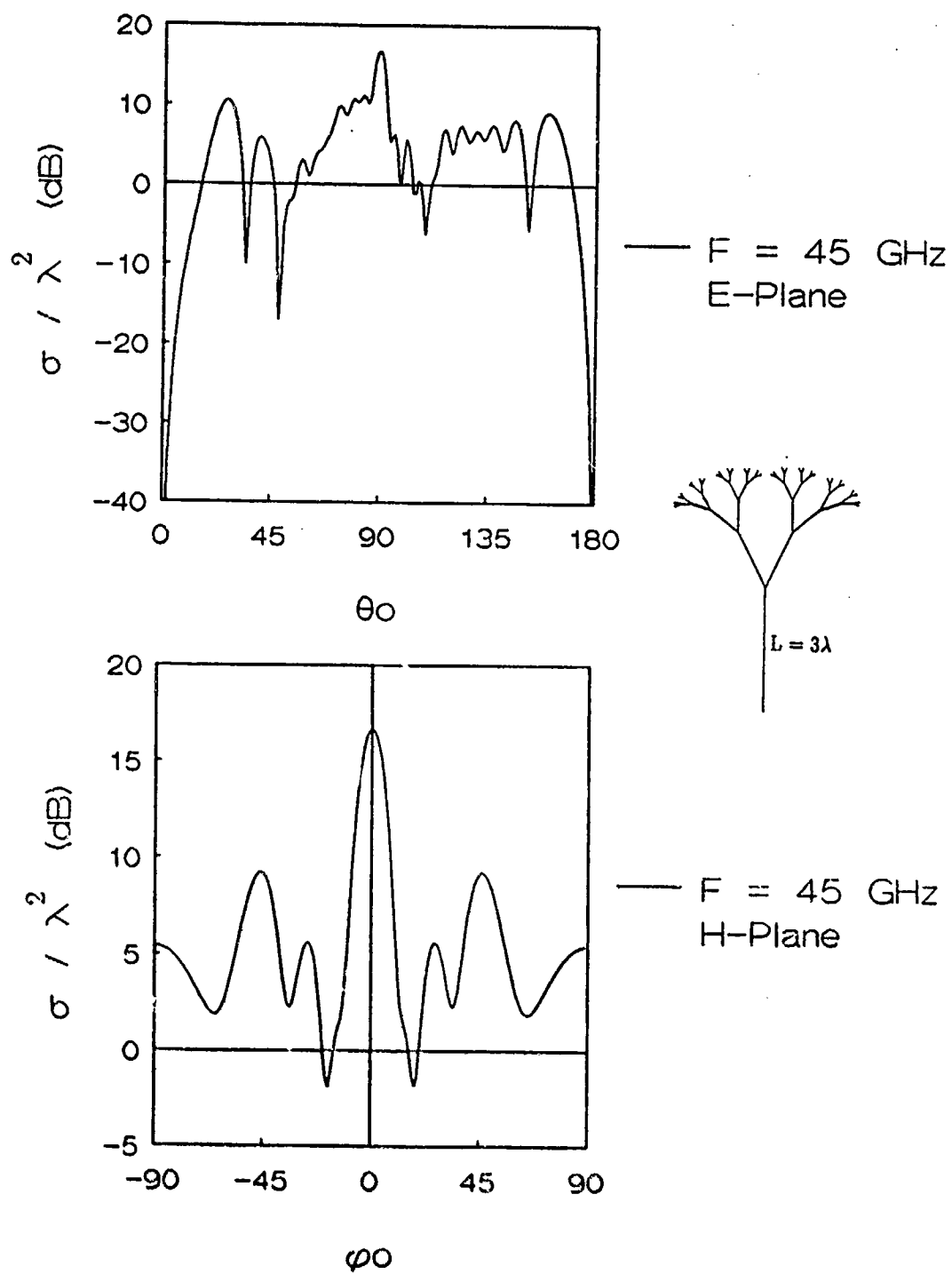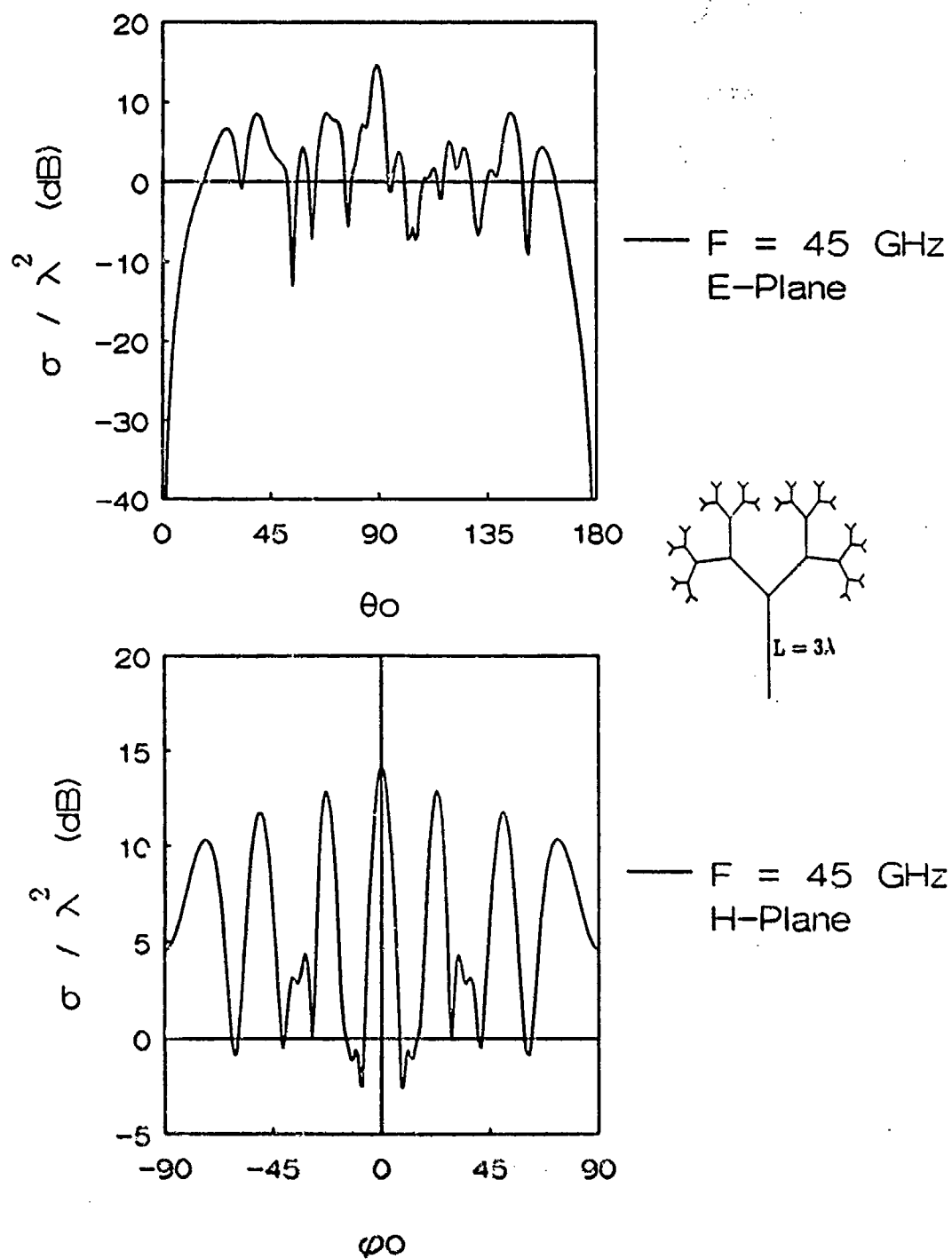
with r = 0.60 and θ = 95.89°.

Figure 5.16 Normalized RCS at F = 45 GHz of a Planar Fractal Tree
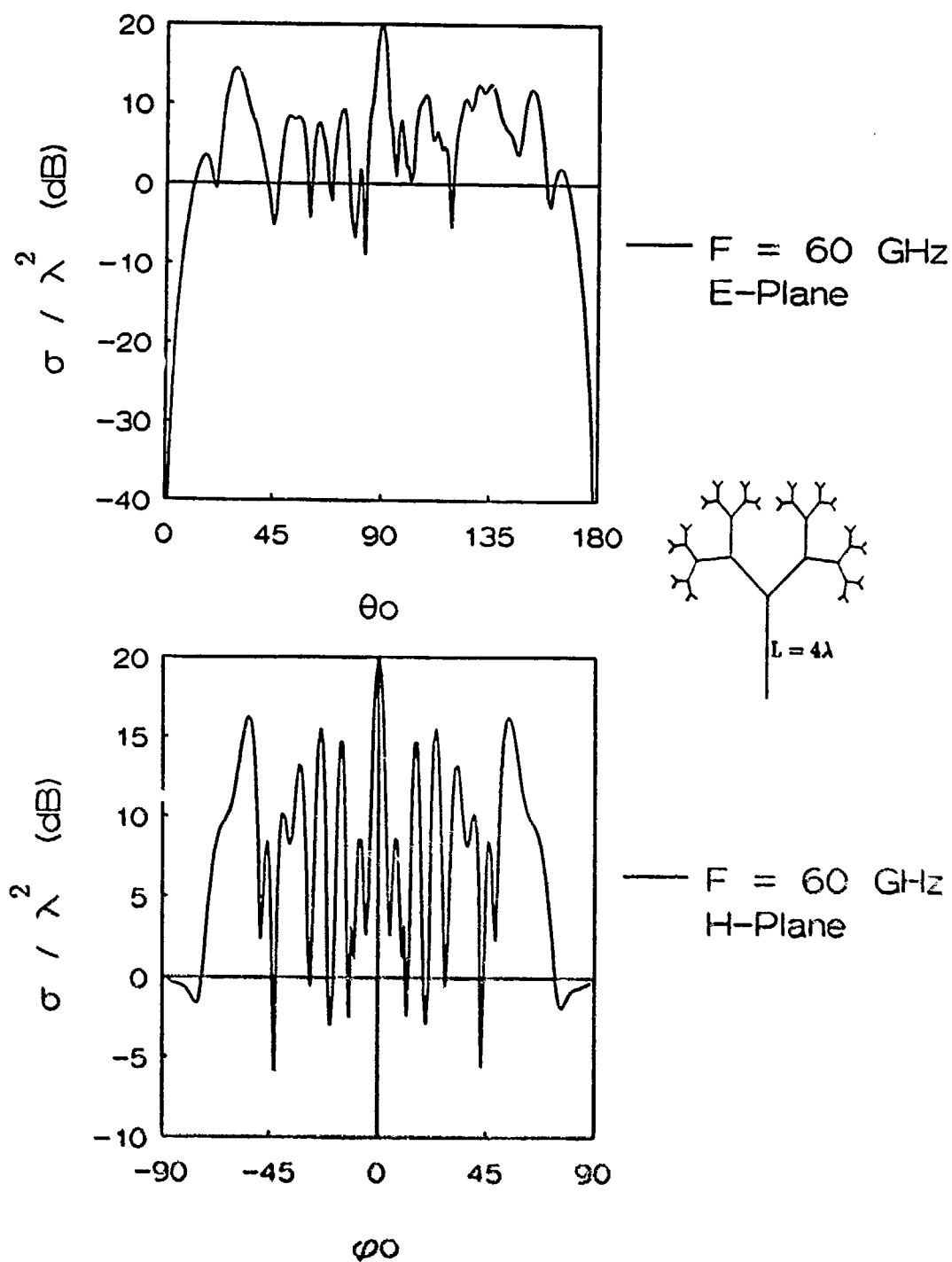
with r = 0.60 and θ = 95.89°.

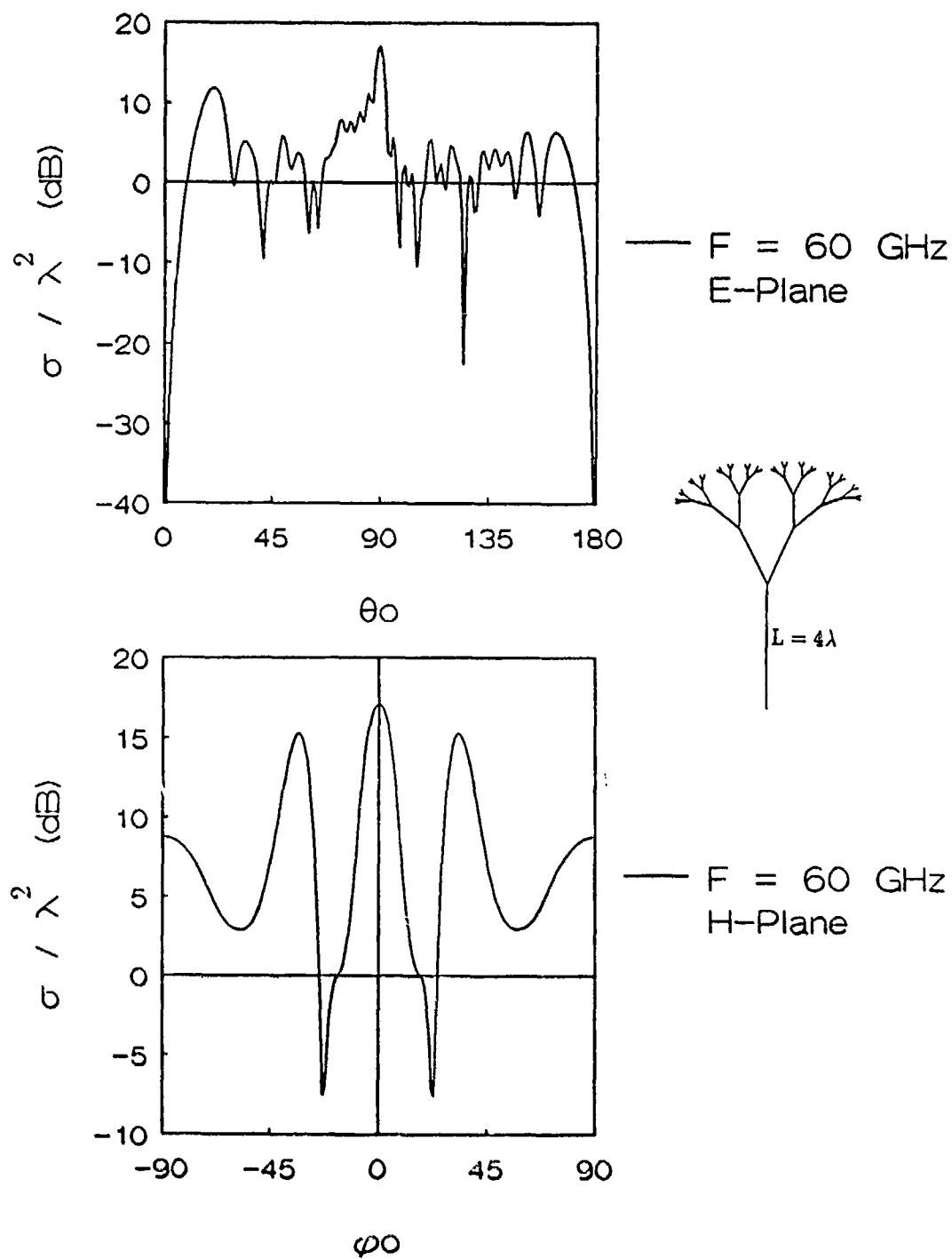Figure 5.17 Normalized RCS at F = 60 GHz of a Planar Fractal Tree
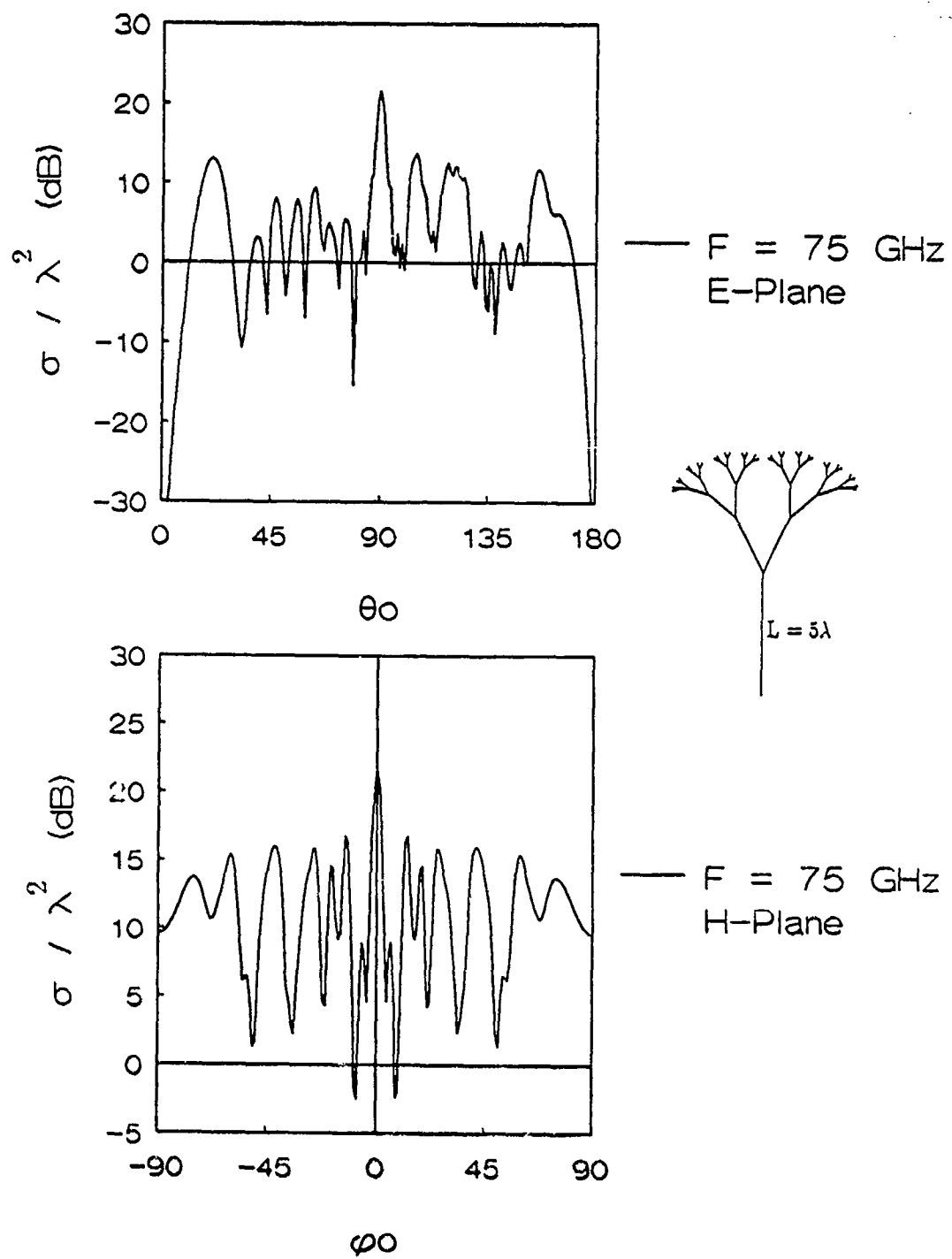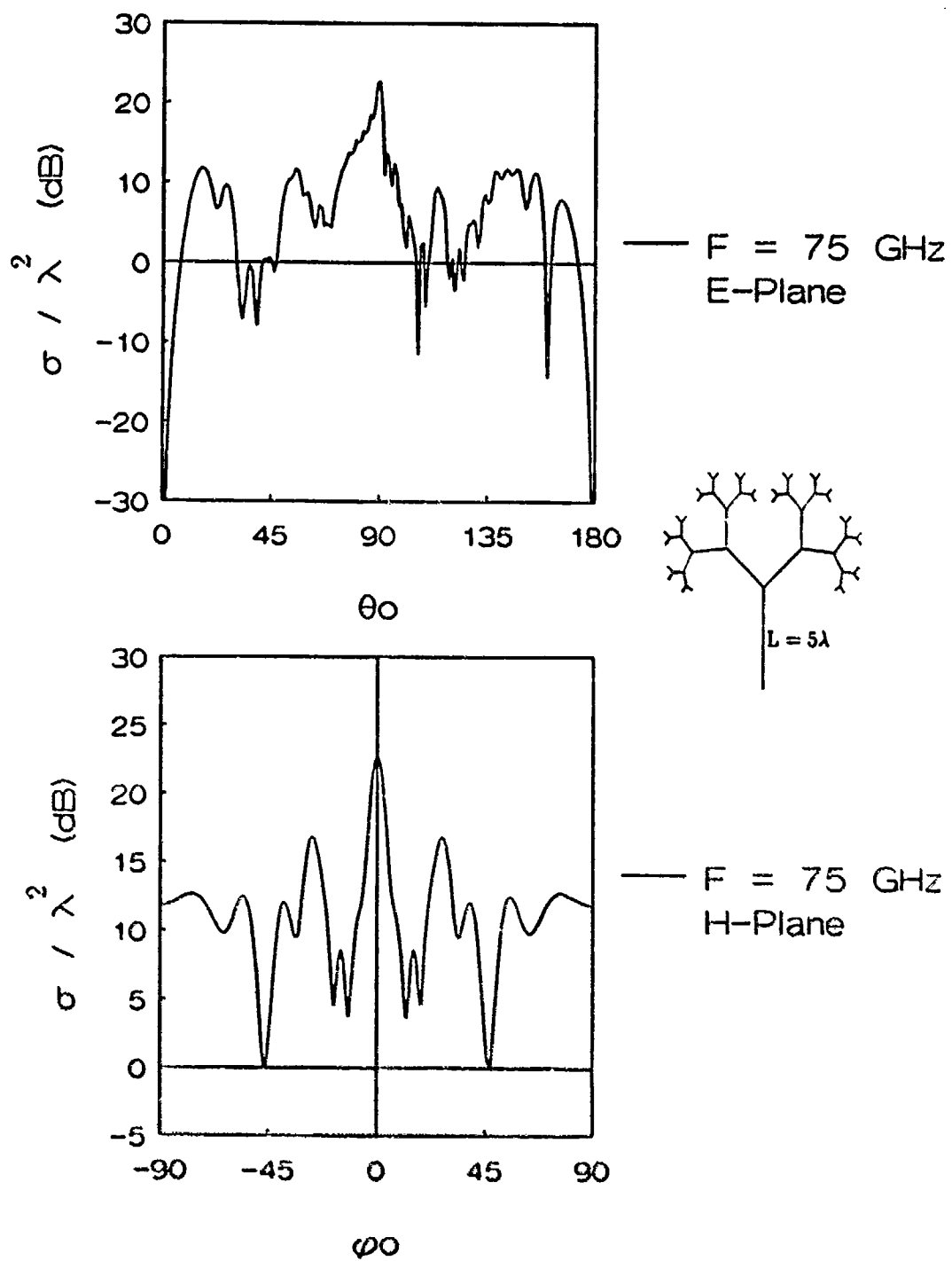
with r = 0.60 and $\theta = 95.89^{o}$.

Figure 5.18 Normalized RCS at F = 75 GHZ of a Planar Fractal Tree

with r = 0.60 and $\theta = 95.89^0$.

62
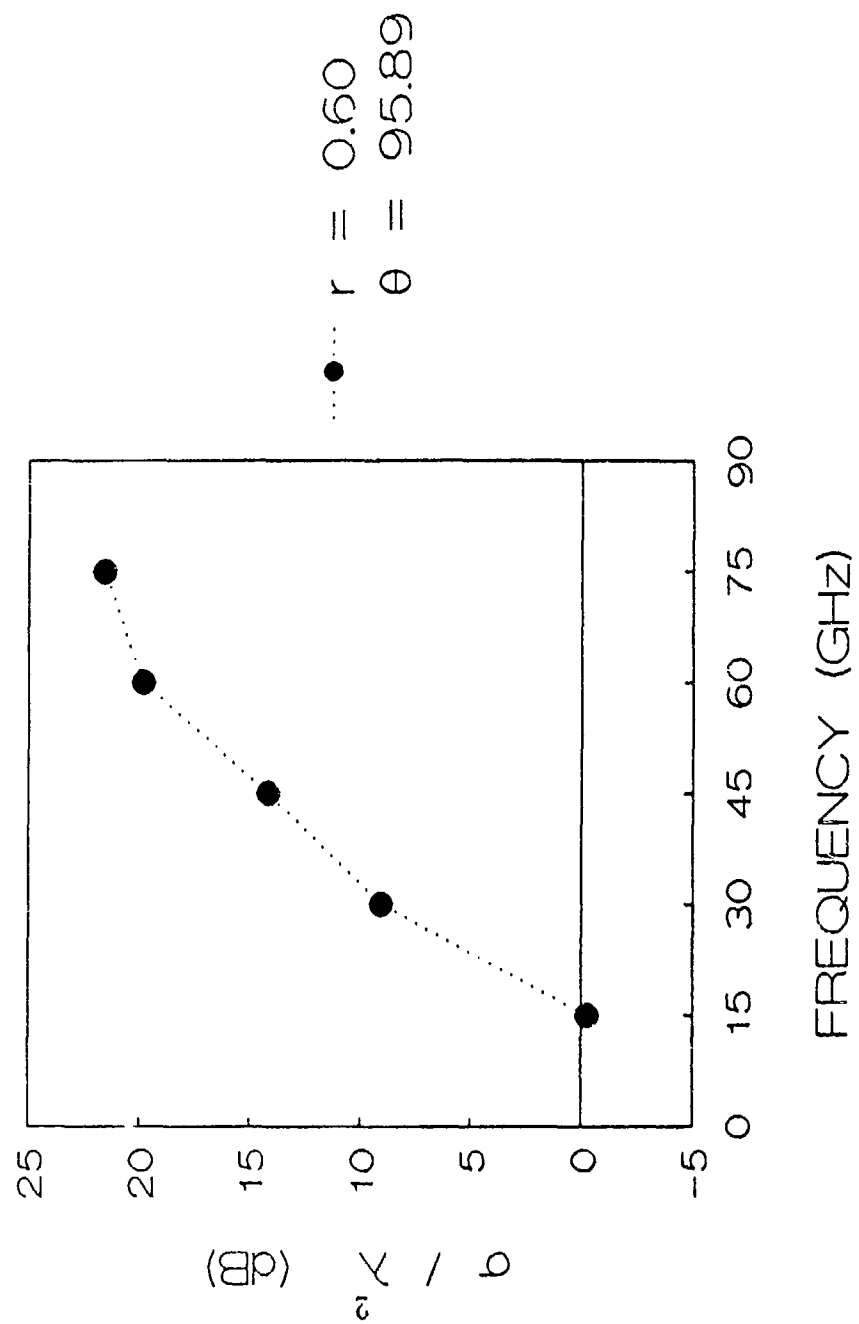
Figure 5.19 Variation of Maximum RCS vs. Frequency

of a Planar Fractal Tree with r = 0.60 and θ = 95.89°.

VI. CONCLUSIONS AND RECOMMENDATIONS

The radar cross section of natural trees is a complicated problem of electromagnetic scattering. The real trees are made up of long, intersecting, and lossy objects. The geometry of these objects is not easy to set up in a three dimensional space.

In this thesis, the real fractal trees were approximated by planar fractal trees. The radar cross section of these trees was calculated by developing a Fortran program. The planar fractal trees that were used for this investigation were symmetric planar structures composed of perfectly conducting and non–intersecting planar dipoles. The geometry of these structures was generated using fractal theory.

A.   CONCLUSIONS

The radar cross section of the planar fractal trees was calculated using the moment method theory. For a given planar structure composed of planar strips and illuminated by a plane wave, the program generates the geometry of the PWS modes, calculates the impedance between any two of them, and fills the impedance matrix [Z]. The voltage on each PWS mode, due to the incident electric field, is also calculated, and the voltage column vector [V] is generated.

The RCS program uses the moment method theory to calculate the current distribution on each PWS mode. The radiation equations of electromagnetic theory are used to determine the scattered electric field due to the current induced on each PWS mode of the structure. The knowledge of both the given incident

electric and calculated scattered electric fields leads to the calculation of the radar cross section (σ/λ^2), for the given angles θ_0, φ_0 of the incident electric field.

The calculated radar cross section of a single centered loaded vertical dipole was compared with the values given in [Ref. 8, pp. 115], for a similar dipole. Although the investigation was for a planar dipole and in [Ref. 8] the dipole was cylindrical, the discrepancy of the results was very small.

In this thesis, five models of planar fractal trees were investigated. The geometry of these models was generated by a given program which was modified to generate the input data for the developed RCS program.

The broadside radar cross section, for the monostatic case, was calculated for three of these planar fractal trees, for a frequency range of 15 GHz to 75 GHz in steps of 15 GHz. This investigation showed that the radar cross section varied in a range of 10 dB in the E–Plane. In the H–Plane, the variation of σ/λ^2 was symmetric about the 90^0 axis and smooth at low frequencies and small branching angles. For higher branching angles and reduction factors, more variations of σ/λ^2 with the frequency were seen in both the E and H planes.

The maximum RCS at $\theta_0 = 90^0$, $\varphi_0 = 0^0$ showed a small variation over a frequency range. This range was different on each investigated tree. The variation of the maximum RCS followed a straight line at the other frequencies. In each tree and at the same frequency, the maximum RCS varied in the range of 3 dB approximately.

It was found that the developed RCS program was not able to calculate the radar cross section of fractal trees that were characterized by large values of reduction factor and branching angle due to memory restrictions and other numerical problems.

The scattering from an actual tree will not exactly follow the patterns that were described in Chapter 5, but it is felt that the trends would generally remain the same. This is specially true for the frequency behavior.

B. RECOMMENDATIONS

One recommendation is to investigate the radar cross section of planar fractal trees characterized by values other than those used in this thesis. Especially, a limited set of reduction factor and branching angle has to be established for the same physical length of the initial dipole.

Another recommendation is to investigate the radar cross section of planar fractal trees characterized by the same values of reduction factor and branching angles as those that were used in this thesis but with different physical and electrical dimensions of the fractal trees.

In this thesis, the branches of the fractal trees were assumed to be perfectly conducting planar strips. The trees were considered without leaves. The radar cross section of fractal trees composed of lossy planar strips and with leaves should be investigated.

Finally, the generation of a three dimensional fractal tree and its radar cross section may be investigated.

APPENDIX A

PROGRAM RCS

```
C
C      THIS PROGRAM CALCULATES THE RADAR CROSS SECTION OF A
C      PLANAR STRUCTURE COMPOSED OF ARBITRARILY ORIENTED
C      PLANAR THIN DIPOLES. THE DIPOLES ARE NOT INTERSECTING.
C      THE DIPOLES ARE PERFECT CONDUCTORS.
C
C
C      GEOMETRY IN Y-Z PLANE
C
C      INPUT DATA:
C
C      F = FREQUENCY IN GHZ
C      NW = NUMBER OF DIPOLES
C      A,B = COORDINATES OF INCIDENT ELECTRIC FIELD ON Y AND Z
C            AXIS RESPECTIVELY.
C      LW  = HALF LENGTH OF EACH DIPOLE IN CM
C      WW =  HALF WIDTH OF EACH DIPOLE IN CM
C      SW, TW = COORDINATES OF THE CENTER OF EACH DIPOLE
C      ALONG Y AND Z AXIS RESPECTIVELY
C      PSIW = ANGLE IN DEGREES BETWEEN THE Z AXIS (REFERENCE)
C             AND DIRECTION OF CURRENT FLOW ON EACH  DIPOLE
C               (POSITIVE ANGLES ARE MEASURED CLOCKWISE)
C      NW = NUMBER OF SEGMENTS THAT EACH DIPOLE IS
C      SUBDIVIDED
C      THITA0, PHI0 = ANGLES IN DEGREES OF INCIDENT ELECTRIC
C      FIELD.
C
C      OUTPUT DATA:
C
C      NORMALIZED RCS (σ/λ²) IN dB
C
      REAL  LS(1:230),S(1:230),T(1:230),PSI(1:230)
      REAL  LEN,PG,SU,TU,WID,A,B,MAG(1:230)
      INTEGER  I,NMAX,INDX(230),NT,NP,L,M,N,K,NW
      COMPLEX Z(1:230,1:230),V(1:230),CUR(1:230)
      COMMON/ RC1/ NMAX
      COMMON/ RC2/ LS,WI,S,T,PSI
      COMMON/ RC4/ CUR
      OPEN (UNIT=1,FILE='INPUT1',FORM='FORMATTED')
      OPEN (UNIT=2,FILE='OUTPUT1',FORM='UNFORMATTED')
      OPEN (UNIT=3,FILE='INPUT',FORM='FORMATTED')
      OPEN (UNIT=4,FILE='OUTPUT',FORM='FORMATTED')
```

```fortran
      READ(1,*) F,NW,A,B
      PI = 4.* ATAN(1.)
      K0 = PI*F/15.
      RAD = PI/180.
      CALL ZMATR (F,NW,Z)
      NP=230
      NT=NMAX
      CALL CLUDCP (Z,NT,NP,INDX)
22    READ (3,*,END=11) THITA0,PHI0
      CALL VOLT(F,THITA0,PHI0,A,B,V)
      CALL CLUBSB (Z,NT,NP,INDX,V)
      DO 54 K=1,NT
      CUR(K)=V(K)
54    CONTINUE
      CALL RADIAT (F,THITA0,PHI0,NMAX,A,B,RCS)
      WRITE(4,*) THITA0,PHI0,RCS
      PRINT*,RCS
      GOTO 22
11    CLOSE(3)
      STOP
      END
C
C
C     SUBROUTINE TO COMPUTE THE MUTUAL IMPEDANCE BETWEEN
C     THE PWS MODES OF N ARBITRARILY ORIENTED DIPOLES.
C
C     GEOMETRY IN THE Y-Z PLANE
C
      SUBROUTINE ZMATR (F,NW,Z)
      REAL F,S(1:230),T(1:230),LG,SG,TG,WI(1:230),PSI(1:230)
      REAL PSIG,PSIW(1:70),LW(1:70),H,W,DH,DW,WIDTH,LENG
      REAL H1,H2,W1,W2,S1,S2,T1,T2,PSI1,PSI2,LS(1:230)
      REAL WW(1:70),SW(1:70),TW(1:70),SS(1:20),TS(1:20)
      REAL PG,WID,LEN,SU,TU,A,B
      INTEGER TEMP,P,L,NS(1:70),NMAX,I,N,NW
      INTEGER FUN,G,J,GB,GR,K
      COMPLEX Z12,Z(1:230,1:230)
      COMMON/ RC2/ LS,WI,S,T,PSI
      COMMON/ RC1/ NMAX
      COMMON/ JOHN/ LG,NG,SG,TG,PSIG,LENG
      COMMON/ ZPAR/ H,W,DW,DH
      COMMON/ ZINC/ H1,H2,W1,W2,S1,S2,T1,T2,PSI1,PSI2
      DO 101 I = 1, NW
      READ(1,*) LW(I),WW(I),SW(I),TW(I),PSIW(I),NS(I)
101   CONTINUE
      CLOSE(1)
      NMAX = 0
      DO 75 I=1,NW
      NMAX = NMAX + (NS (I) - 1)
75    CONTINUE
      P=1
      GB=0
```

```fortran
      DO 50 I=1,NW
              LENG = LW(I)
              LG=2*LW(I)/FLOAT(NS(I))
              WIDTH=WW(I)
              NG=NS(I)
              SG=SW(I)
              TG=TW(I)
              PSIG=PSIW(I)
              CALL GEOM(SS,TS)
              GR=NS(I)+GB-1
              M = P
              DO 60 J=1,NS(I)-1
                      PSI(M)=PSIG
                      LS(M)=LG
                      WI(M)=WIDTH
                      S(M)=SS(J)
                      T(M)=TS(J)
                      PRINT*,S(M),T(M)
                      M = M + 1
60            CONTINUE
              GB=GR
              P=GR+1
50    CONTINUE
      TEMP=NS(1)-1
      L=1
      G=NMAX
      DO 80 M=1,G
              IF(M.LE.TEMP)GOTO 85
              L=L+1
              TEMP=TEMP+NS(L)-1
85            CONTINUE
              K=TEMP
              DO 90 N=M,G
                      IF(N.LE.K)THEN
                      H=LS(M)
                      W=WI(M)
                      DW=0
                      DH=ABS(M-N)*H
                      CALL ZSDIP(F,Z12)
                      Z(M,N)=Z12
                      PRINT*,Z(M,N)
                      WRITE(2) Z(M,N)
                      ELSE
                      H1=LS(M)
                      H2=LS(N)
                      W1=WI(M)
                      W2=WI(N)
                      S1=S(M)
                      S2=S(N)
                      T1=T(M)
```

```fortran
                    T2=T(N)
                    PSI1=PSI(M)
                    PSI2=PSI(N)
                    CALL ZPSUR (F,Z12)
                    Z(M,N)=Z12
                    PRINT*,Z(M,N)
                    WRITE(2) Z(M,N)
                    ENDIF
90            CONTINUE
80      CONTINUE
        DO 24 M=2,G
            DO 26 N=1,M-1
                    Z(M,N)=Z(N,M)
                    WRITE(2) Z(M,N)
26          CONTINUE
24      CONTINUE
        RETURN
        END
C
C       SUBROUTINE TO COMPUTE THE MUTUAL/SELF IMPEDANCE
C       BETWEEN TWO DIPOLES. THE DIPOLES ARE ASSUMED TO BE
C       COPLANAR, IDENTICAL AND PARALLEL. THE DIPOLE TO
C       DIPOLE IMPEDANCE IS COMPUTED AS THE SUM OF FOUR
C       MONOPOLE TO MONOPOLE IMPEDANCES.
C
C       INPUT PARAMETERS:
C
C       F = Frequency of operation (GHz)
C       H = Half height of the dipole (cm)
C       W = Half width of the dipole (cm)
C       DH = Longitudinal distance between the two dipoles (cm)
C       DW = Transverse distance between the two dipoles (cm)
C
        SUBROUTINE ZSDIP (F,Z12)
        REAL  H, W, DW, DH, F
        COMPLEX  Z12, ZT
        COMMON/ ZPAR/ H,W,DW,DH
        ZT = (0.,0.)
        Z12 = (0.,0.)
        CALL ZSMONP (F, H, W, DW, DH, 0, 1, 0, 1, ZT)
        Z12 = Z12 + ZT
        CALL ZSMONP (F, H, W, DW, DH + H, 0, 1, 1, 0, ZT)
        Z12 = Z12 + ZT
        CALL ZSMONP (F, H, W, DW, DH - H, 1, 0, 0, 1, ZT)
        Z12 = Z12 + ZT
        CALL ZSMONP (F, H, W, DW, DH, 1, 0, 1, 0, ZT)
        Z12 = Z12 + ZT
        RETURN
        END
```

```
C     SUBROUTINE TO COMPUTE THE SELF/MUTUAL IMPEDANCE
C     BETWEEN TWO IDENTICAL, COPLANAR MONOPOLES. THE
C     CURRENT IS ASSUMED TO BE CONSTANT IN THE
C     TRANSVERSE DIRECTION.
C
C     REF:  R. JANASWAMY, A SIMPLIFIED EXPRESSION FOR THE
C           SELF/MUTUAL IMPEDANCE BETWEEN TWO COPLANAR
C           AND PARALLEL MONOPOLES, IEEE T-AP, AP-35,
C           No. 10, pp. 1174-1176, October 1987.
C
C     INPUT PARAMETERS:
C
C     F = FREQUENCY IN GHz
C     H = LENGTH OF EACH MONOPOLE (cm)
C     W = WIDTH OF EACH MONOPOLE  (cm)
C     D = CENTER TO CENTER SPACING BETWEEN THE TWO
C     MONOPOLES IN THE DIRECTION TRANSVERSE TO THE
C     CURRENT FLOW (cm)
C     HH = CENTER TO CENTER SPACING BETWEEN THE TWO
C     MONOPOLES IN THE DIRECTION OF CURRENT FLOW (cm)
C
C     I11 = TERMINAL CURRENT OF END 1 OF MONOPOLE 1.
C     I21 = TERMINAL CURRENT OF END 2 OF MONOPOLE 1.
C     I12 = TERMINAL CURRENT OF END 1 OF MONOPOLE 2.
C     I22 = TERMINAL CURRENT OF END 2 OF MONOPOLE 2.
C
C     NOTE:       I11, I21, I12, I22 can assume values only 0 or 1.
C     ICODE = 0, IF  D .LE. 4W
C     ICODE = 1, OTHERWISE
C     With ICODE = 0, the expression provided in the above paper is used.
C     With ICODE = 1, a modified form of the expression provided in the
C     above paper is used. (cf. notes)
C
C     OUTPUT PARAMETERS:
C
C     Z12 = COMPLEX IMPEDANCE BETWEEN THE TWO SURFACE
C     MONOPOLES.
C
      SUBROUTINE ZSMONP (F, H, W, D, HH, I11, I21, I12, I22, Z12)
      REAL F, H, W, D, HH, A, B, PI, K0, V, UB, UBP, UA, UAP
      REAL KW, KH, KD, RC, FR, FI, I1, I2, I3, I4, SI, CI
      REAL UABP, ZR, ZI, X, AA (1), BB (1), SQXV, UAB, TINY
      INTEGER I11, I21, I12, I22, M, N, NX, KI, ICODE
      COMPLEX Z12, AC (-1:1, -1:1), E1, E2, Z1, J, CMN, E3, EI, FAC
      EXTERNAL FR, FI
      COMMON /PARAM/ N, V, KD, A, B, ICODE
      EI (X) = CI (ABS (X)) - J * SI (X)
      SQXV (X) = SQRT (X * X + V * V)
      TINY = 1.E-6
      PI = 4. * ATAN (1.)
      NX = 1
```

```
            K0 = PI * F / 15.
            KW = K0 * W
            KH = K0 * H
            KD = K0 * D
            ICODE = 0
            IF (KD .GT. 4. * KW) ICODE = 1
            KI = 10
C
C     Note that with this choice of KI accurate results are found in the
C     region 0 < D < 4 W, and for D > 20 W. In between these two regions,
C     accurate results are found with KI = 20. Hence the above choice is
C     good only if this code is used for values of D satisfying the above
C     inequalities.
C
            FAC = CMPLX (1., 0.)
            A = KD - 2. * KW
            B = KD + 2. * KW
            IF (ICODE .EQ. 1) GO TO 2
            AA (1) = A
            BB (1) = B
            GO TO 3
2           AA (1) = -2. * KW
            BB (1) = 2. * KW
3           I1 = (I21 * COS (KH) - I11) * I12
            I2 = (I11 - I21 * COS (KH)) * I22
            I3 = (I21 - I11 * COS (KH)) * I12
            I4 = (I21 - I11 * COS (KH)) * I22
            J = CMPLX (0.,1.)
            Z1 = CEXP (J * KH)
            AC (-1, -1) = I2 + I1 / Z1
            AC (-1, 1) = I2 + I1 * Z1
            AC (1, -1) = I3 - I4 * Z1
            AC (1, 1) = I3 - I4 / Z1
            AC (0, -1) = - (AC (-1, -1) * Z1 + AC (1, -1) / Z1)
            AC (0, 1) = - (AC (1, 1) * Z1 + AC (-1, 1) / Z1)
            RC = 15. / (2. * SIN (KH) * KW) ** 2
            Z12 = (0., 0.)
            DO 1 M = -1, 1
            DO 1 N = -1, 1, 2
            V = K0 * (HH + M * H)
            IF (ICODE .EQ. 0) GO TO 4
            FAC = CEXP (J * N * V)
            CMN = CMPLX (0.,0.)
            GO TO 5
4           UA = SQXV (A) + N * V
            UAP = UA - 2. * N * V
            UB = SQXV (B) + N * V
            UBP = UB - 2. * N * V
            UAB = SQXV (KD) + N * V
            UABP = UAB - 2. * N * V
            E1 = EI (UB)
```

```fortran
      E2 = (0.,0.)
      IF (ABS (A) .GT. TINY) E2 = EI (UA)
      E3 = (0.,0.)
      IF (ABS (KD) .GT. TINY) E3 = EI (UAB)
      CMN = 0.5 * (B * B * E1 + A * A * E2 - 2. * KD * KD * E3 +
     &     CEXP (-J * UB) * (1. + J * UBP) + CEXP (-J * UA) *
     &     (1. + J * UAP) - 2. * CEXP (- J * UAB) * (1. + J * UABP))
    5 CALL HABER (NX, AA, BB, FR, KI, ZR)
      CALL HABER (NX, AA, BB, FI, KI, ZI)
      Z12 = Z12 + AC (M, N) * (CEXP (J * N * V) * CMN + (ZR + J * ZI)
     &        * FAC)
    1 CONTINUE
      Z12 = Z12 * RC
      RETURN
      END
C
      REAL FUNCTION FR (XI, NX)
      INTEGER N, NX, CODE
      REAL X, V, T1, KD, A, B, XI (NX), TKW, T2, CI, SI, TINY
      COMPLEX EI, J
      COMMON /PARAM/ N, V, KD, A, B, CODE
      EI (X) = CI (ABS (X)) - J * SI (X)
      TINY = 1.E-6
      X = XI (1)
      J = CMPLX (0.,1.)
      IF (CODE .EQ. 1) GO TO 1
      T1 = SQRT (X * X + V * V)
      FR = COS (T1)
      IF (ABS (V) .GT. TINY) FR = FR * (1. - N * V / T1)
      IF (X .LE. KD) FR = FR * A
      IF (X .GT. KD) FR = -FR * B
      GO TO 2
    1 TKW =  0.5 * (B - A)
      T2 = SQRT ((KD + X) * (KD + X) + V * V)
      FR = REAL (EI (T2 + N * V))
      FR = FR * (TKW - ABS (X))
    2 END


      REAL FUNCTION FI (XI, NX)
      INTEGER N, NX, CODE
      REAL X, V, T1, KD, A, B, XI (NX), TKW, T2, CI, SI  TINY
      COMPLEX EI, J
      COMMON /PARAM/ N, V, KD, A, B, CODE
      EI (X) = CI (ABS (X)) - J * SI (X)
      X = XI (1)
      TINY = 1.E-6
      J = CMPLX (0., 1.)
      T1 = SQRT (X * X + V * V)
      IF (CODE .EQ. 1) GO TO 1
```

```fortran
      FI = -SIN (T1)
      IF (ABS (V) .GT. TINY) FI = FI * (1. - N * V / T1)
      IF (X .LE. KD) FI = FI * A
      IF (X .GT. KD) FI = -FI * B
      GO TO 2
   1  TKW =  0.5 * (B - A)
      T2 = SQRT ((KD + X) * (KD + X) + V * V)
      FI = AIMAG (EI (T2 + N * V))
      FI = FI * (TKW - ABS (X))
   2  END
C
C     SUBROUTINE TO COMPUTE THE COORDINATES OF THE PWS
C     MODES OF EACH DIPOLE IN THE Y-Z PLANE
C
      SUBROUTINE GEOM (S,T)
      REAL THI,H1,H2,Y,Z,SG,TG,LG,PSIG
      REAL P,Q,S(1:20),T(1:20),LENG
      INTEGER M,NG,K
      COMMON/ JOHN/ LG,NG,SG,TG,PSIG,LENG
      COSD(X) = COS(X*RAD)
      SIND(X) = SIN(X*RAD)
      PI=4.*ATAN(1.)
      RAD=PI/180.
      THI=90.-PSIG
      H1=COSD(THI)
      H2=SIND(THI)
      Y=SG-(LENG*H1)
      Z=TG-(LENG*H2)
      P=LG*H1
      Q=LG*H2
      S(1)=Y+P
      T(1)=Z+Q
      DO 225 K=2,NG-1
           S(K)=S(1)+(K-1)*P
           T(K)=T(1)+(K-1)*Q
  225 CONTINUE
      RETURN
      END
C
C
      SUBROUTINE  ZPSUR (F,Z12)
      REAL H1, W1, H2, W2, PSI, F, YSTAR, ZSTAR, K0, AI (2), BI (2)
      REAL C (3), D (3), RT, ZT, COT, CSEC, KOS, X, PI, PSI1, PSI2
      REAL S1, T1, S2, T2, RINTG, IMINTG, RESULT, SIND, COSD,SI,CI
      INTEGER NX, KI
      COMPLEX Z12, J
      EXTERNAL RINTG, IMINTG
      COMMON/ ZINC/ H1,H2,W1,W2,S1,S2,T1,T2,PSI1,PSI2
      COMMON /PARAM2/ C, D, RT, ZT, CSEC, COT, KOS, J, K0
      SIND (X) = SIN (X * PI / 180.)
```

```fortran
      COSD (X) = COS (X * PI / 180.)
      DATA AI, BI /2 * -1., 2 * 1./
      PI = 4. * ATAN (1.)
      PSI = PSI2 - PSI1
      IF (ABS (PSI).LE.0.4) PSI= SIGN(1.,PSI)*0.4
      J = CMPLX (0.,1.)
      NX = 2
      KI = 3
      K0 = PI * F / 15.
      C (1) = 1. / SIN (K0 * H1)
      C (3) = C (1)
      C (2) = -2. * COS (K0 * H1) * C (1)
      D (1) = 1. / SIN (K0 * H2)
      D (3) = D (1)
      D (2) = -2. * COS (K0 * H2) * D (1)
      CSEC = 1. / SIND (PSI)
      KOS = COSD (PSI)
      COT = KOS * CSEC
      YSTAR = (S2-S1) * COSD (PSI1) - (T2-T1) * SIND (PSI1)
      ZSTAR = (S2-S1) * SIND (PSI1) + (T2-T1) * COSD (PSI1)
      RT = YSTAR * CSEC - H2
      ZT = YSTAR * COT - H1 - ZSTAR
      CALL HABER (NX, AI, BI, RINTG, KI, RESULT)
      Z12 = RESULT
      CALL HABER (NX, AI, BI, IMINTG, KI, RESULT)
      Z12 = Z12 + J * RESULT
      Z12 = -3.75 * Z12
      RETURN
      END
C
      REAL FUNCTION SI (XI)
      REAL XI
      REAL AF (4), BF (4), AG (4), BG (4), X, X2, X4, X6, X8, FX, GX,
     &     PI, SGN
      DATA  AF / 38.027264, 265.187033, 335.67732, 38.102495 /
      DATA  BF / 40.021433, 322.624911, 570.23628, 157.105423 /
      DATA  AG / 42.242855, 302.757865, 352.018498, 21.821899 /
      DATA  BG / 48.196927, 482.485984, 1114.978885, 449.690326 /
      SI = 0.
      IF (XI .EQ. 0.) RETURN
      SGN = +1.
      IF (XI .LT. 0.) SGN = -1.
      X = ABS (XI)
      X2 = X * X
      IF (X .GE. 20.) THEN
      FX = 1. / X * (1. - 2. / X2)
      GX = 1. / X2 * (1. - 6. / X2)
      GO TO 1
      END IF
      X4 = X2 * X2
      X6 = X4 * X2
```

```fortran
      X8 = X4 * X4
      IF (X .LT. 1.) THEN
      SI = X*(1. -- X2 / 18. + X4 / 600. - X6 / 35280. + X8 / 3265920.)
      SI = SI * SGN
      ELSE
    & FX = (1. + AF (1) / X2 + AF (2) / X4 + AF (3) / X6 + AF (4) /
          X8)
    & FX = FX / (X * (1. + BF (1) / X2 + BF (2) / X4 + BF (3) / X6 +
          BF (4) / X8))
    & GX = (1. + AG (1) / X2 + AG (2) / X4 + AG (3) / X6 + AG (4) /
          X8)
    & GX = GX / (X2 * (1. + BG (1) / X2 + BG (2) / X4 + BG (3) / X6 +
          BG(4) / X8))
    1 PI = 4. * ATAN (1.)
      X = X - AINT (X / (2. * PI)) * 2. * PI
      SI = SGN * (PI / 2. - FX * COS (X) - GX * SIN (X))
      END IF
      END
C
C

      REAL FUNCTION CI (X)
      REAL AF (4), BF (4), AG (4), BG (4), X, X2, X4, X6, X8, FX, GX
      REAL PI
      DATA  AF / 38.027264, 265.187033, 335.67732, 38.102495 /
      DATA  BF / 40.021433, 322.624911, 579.23628, 157.105423 /
      DATA  AG / 42.242855, 302.757865, 352.018498, 21.821899 /
      DATA  BG / 48.196927, 482.485984, 1114.978885, 449.690326 /
      IF (X .LE. 0.)THEN
      PRINT *, 'Invalid argument for CI (x)', ' x = ', x
      RETURN
      ELSE
      X2 = X * X
      X4 = X2 * X2
      IF (X .GE. 20.) THEN
      FX = 1. / X * (1. - 2. / X2)
      GX = 1. / X2 * (1. - 6. / X2)
      GO TO 1
      END IF
      X6 = X4 * X2
      X8 = X4 * X4
      IF (X .LT. 1.) THEN
    & CI = 0.57721566 + ALOG (X) - X2 * (0.25 - X2 / 96. + X4 / 4320.
          - X6 / 322560.)
      ELSE
    & FX = (1. + AF (1) / X2 + AF (2) / X4 + AF (3) / X6 + AF (4) /
          X8)
    & FX = FX / (X * (1. + BF (1) / X2 + BF (2) / X4 + BF (3) / X6 +
          BF (4) / X8))
    & GX = (1. + AG (1) / X2 + AG (2) / X4 + AG (3) / X6 + AG (4) /
          X8)
      GX = GX / (X2 * (1. + BG (1) / X2 + BG (2) / X4 + BG (3) / X6 +
```

```
&              BG(4) / X8))
1      PI = 4. * ATAN (1.)
       X = X − AINT (X / (2. * PI)) * 2. * PI
       CI = FX * SIN (X) − GX * COS (X)
       END IF
       END IF
       END
C
       REAL FUNCTION RINTG (X, NX)
       COMPLEX J, EI, TERM1, TERM2, INTGR
       INTEGER NX, M, N, P, Q
       REAL * 4 PSI1, PSI2, S1, T1, S2, T2
       REAL * 4 C (3), D (3), R, Z, RT, ZT, U, V, CSEC, COT, KOS, Y
       REAL * 4 X (NX), H1, H2, W1, W2, K0, PZQR, SI, CI
&              ,TT, ZM, RN, RMN, TESC, TESD, PI, PZQRP
       COMMON/ ZINC/ H1,H2,W1,W2,S1,S2,T1,T2,PSI1,PSI2
       COMMON /PARAM2/ C, D, RT, ZT, CSEC, COT, KOS, J, K0
       EI (Y) = CI (ABS(Y)) − J * SI (Y)
       U = X (1)
       V = X (2)
       INTGR = (0.,0.)
       TESC = ABS (C (2) / C (1))
       TESD = ABS (D (2) / D (1))
       TT = ALOG (ABS ((1.+KOS)/(1.−KOS)))
       PI = 4. * ATAN (1.)
       DO 3 M = 1, 3
       IF (M .EQ. 2 .AND. TESC .LE. 1.E−6) GO TO 3
       Z = (M−1) * H1
       ZM = −U * W1 * COT + V * W2 * CSEC + ZT + Z
       TERM2 = (0.,0.)
       DO 2 N = 1, 3
       IF (N .EQ. 2 .AND. TESD .LE. 1.E−6) GO TO 2
       R = (N−1) * H2
       RN = −U * W1 * CSEC + V * W2 * COT + RT + R
       IF (ABS (K0 * RN) .LE. 0.5E−1) THEN
       PZQRP = K0 * ABS (ZM) − AINT (K0 * ABS (ZM) / (2. * PI)) *
&              2. * PI
       TERM1 = CEXP (−J * PZQRP) * TT
       GO TO 4
       END IF
       IF (ABS (K0 * ZM) .LE. 0.5E−1) THEN
       PZQRP = K0 * ABS (RN) − AINT (K0 * ABS (RN) / (2. * PI)) *
&              2. * PI
       TERM1 = CEXP (−J * PZQRP) * TT
       GO TO 4
       END IF
       RMN = SQRT (RN * RN + ZM * ZM − 2. * RN * ZM * KOS)
       TERM1 = (0.,0.)
       DO 1 P = −1, 1, 2
       DO 1 Q = −1, 1, 2
       PZQR = P * ZM + Q * RN
```

77

```fortran
      PZQRP = PZQR * K0 - AINT (PZQR * K0 / (2. * PI)) * 2. * PI
      TERM1 = TERM1 + P * Q * CEXP (J * PZQRP) *
     &        EI (K0 * (RMN + PZQR))
1     CONTINUE
4     TERM2 = TERM2 + D (N) * TERM1
2     CONTINUE
      INTGR = INTGR + C (M) * TERM2
3     CONTINUE
      RINTG = REAL (INTGR)
      END

      REAL FUNCTION IMINTG (X, NX)
      COMPLEX J, EI, TERM1, TERM2, INTGR
      INTEGER NX, M, N, P, Q
      REAL * 4 PSI1, PSI2, S1, T1, S2, T2
      REAL * 4 C (3), D (3), R, Z, RT, ZT, U, V, CSEC, COT, KOS, Y
      REAL * 4 X (NX), H1, H2, W1, W2, K0, PZQR, SI, CI
     &        ,TT, ZM, RN, RMN, TESC, TESD, PI, PZQRP
      COMMON/ ZINC/ H1,H2,W1,W2,S1,S2,T1,T2,PSI1,PSI2
      COMMON /PARAM2/ C, D, RT, ZT, CSEC, COT, KOS, J, K0
      EI (Y) = CI (ABS(Y)) - J * SI (Y)
      U = X (1)
      V = X (2)
      INTGR = (0.,0.)
      TESC = ABS (C (2) / C (1))
      TESD = ABS (D (2) / D (1))
      TT = ALOG (ABS ((1.+KOS)/(1.-KOS)))
      PI = 4. * ATAN (1.)
      DO 3 M = 1, 3
      IF (M .EQ. 2 .AND. TESC .LE. 1.E-6) GO TO 3
      Z = (M-1) * H1
      ZM = -U * W1 * COT + V * W2 * CSEC + ZT + Z
      TERM2 = (0.,0.)
      DO 2 N = 1, 3
      IF (N .EQ. 2 .AND. TESD .LE. 1.E-6) GO TO 2
      R = (N-1) * H2
      RN = -U * W1 * CSEC + V * W2 * COT + RT + R
      IF (ABS (K0 * RN) .LE. 0.5E-1) THEN
      PZQRP = K0 * ABS (ZM) - AINT (K0 * ABS (ZM) / (2. * PI)) *
     &        2. * PI
      TERM1 = CEXP (-J * PZQRP) * TT
      GO TO 4
      END IF
      IF (ABS (K0 * ZM) .LE. .5E-1) THEN
      PZQRP = K0 * ABS (RN) - AINT (K0 * ABS (RN) / (2. * PI)) *
     &        2. * PI
      TERM1 = CEXP (-J * PZQRP) * TT
      GO TO 4
      END IF
      RMN = SQRT (RN * RN + ZM * ZM - 2. * RN * ZM * KOS)
```

```
        TERM1 = (0.,0.)
        DO 1 P = -1, 1, 2
        DO 1 Q = -1, 1, 2
        PZQR = P * ZM + Q * RN
        PZQRP = K0 * PZQR - AINT (K0 * PZQR / (2. * PI)) * 2. * PI
        TERM1 = TERM1 + P * Q * CEXP (J * PZQRP) *
     &          EI (K0 * (RMN + PZQR))
   1    CONTINUE
   4    TERM2 = TERM2 + D (N) * TERM1
   2    CONTINUE
        INTGR = INTGR + C (M) * TERM2
   3    CONTINUE
        IMINTG = AIMAG (INTGR)
        END
C
C
C       Subroutine to compute a sequence of estimates EST1 (K) and
C       EST2 (K), 1 .LE. K1 .LE. K .LE. K2 for the N-dimensional integral
C           B1      BN
C           Int ... Int  FUN (x1, x2, ... xN) dx1 dx2... dx3
C           A1      AN
C       by Haber's method.
C       Ref:    P. J. Davis and P. Rabinowitz, Methods of Numerical
C                   Integratation, Academic Press, 1984.
C
C       For each estimate EST1 (K), two additional quantities ERR1(K)
C       and DEV1 (K) are computed. If the values of DEV1 (K) do not
C       vary by more than 10% between consecutive values of K, then
C       ERR1 (K) can be taken as a reliable bound on the difference
C       between EST1 and the integral. A similar situation holds for
C       EST2, DEV2, and ERR2 (K). The total number of functional
C       evaluations is 4 * (K1 ** N + (K1+1) ** N + ... + K2 ** N) and K2
C       should be chosen so as to make this may be halfed by eliminating the
C       computation of the EST2 (K). In other situations, these values
C       are much better than the EST1 (K). A program FUNCTION FUN (X, N)
C       must be supplied by the user with X declared by the statement
C       DIMENSION X (N). FUN must be declared EXTERNAL in the calling
C       program. If N < 1 or N > 10 or K1 < 1 or K2 < K1, the program
C       terminates with IND = 0. Otherwise IND = 1.
C
C       Modified by R. Janaswamy so that the output is average of EST1
C       EST2. Also, K1 = K2 = K.
C
        SUBROUTINE HABER (N, LL, UL, FUN, K, RESULT)
        INTEGER  N, IND, KEY, I, K, J
        DOUBLE PRECISION  AL (10), BE (10), GA (10), B, G
        REAL FUN, Y1, Y2, Y3, Y4, EST1, EST2, ERR1, ERR2,
     &          DEV1, DEV2, RESULT
        REAL * 8  S1, S2, D1, D2
        REAL LL (N), UL (N), DEX (10), P1 (10), P2 (10), P3 (10), P4 (10),
     &  Q1 (10), Q2 (10), Q3 (10), Q4 (10), RAN (10), AKN, AK, T, JAC
        REAL AK1, BK
```

```
      EXTERNAL FUN
      DATA AL/.4142135623730950, .7320508075688773, .2360679774997897,
&            .6457513110645906, .3166247903553998, .6055512754639893,
&            .1231056256176605, .3589989435406736, .7958315233127195,
&            .3851648071345040/
      IND = 0
      IF (N .LT. 1 .OR. N .GT. 10) RETURN
      IND = 1
      JAC = 1.
      DO 1 I = 1, N
      BE (I) = AL (I)
      GA (I) = AL (I)
      RAN (I) = UL (I) - LL (I)
      JAC = JAC * RAN (I)
1     DEX (I) = 0.
      AK = FLOAT (K)
      KEY = 0
      AK1 = AK - 1.1
      S1 = 0.
      D1 = 0.
      S2 = 0.
      D2 = 0.
      AKN = AK ** N
      T = SQRT (AKN) * AK
      BK = 1. / AK
5     KEY = KEY + 1
      IF (KEY .EQ. 1) GO TO 6
      KEY = KEY - 1
      J = 1
4     IF (DEX (J) .GT. AK1) GO TO 8
      DEX (J) = DEX (J) + 1.
      GO TO 6
8     DEX (J) = 0.
      J = J + 1
      IF (J .LE. N) GO TO 4
      GO TO 3
6     DO 7 I = 1, N
      B = BE (I) + AL (I)
      IF (B .GT. 1.) B = B - 1.
      G = GA (I) + B
      IF (G .GT. 1.) G = G - 1.
      BE (I) = B + AL (I)
      IF (BE (I) .GT. 1.) BE (I) = BE (I) - 1.
      GA (I) = BE (I) + G
      IF (GA (I) .GT. 1.) GA (I) = GA (I) - 1.
      P1 (I) = (DEX (I) + G) * BK
      Q1 (I) = LL (I) + RAN (I) * P1 (I)
      P2 (I) = (DEX (I) + 1. - G) * BK
      Q2 (I) = LL (I) + RAN (I) * P2 (I)
      P3 (I) = (DEX (I) + GA (I)) * BK
      Q3 (I) = LL (I) + RAN (I) * P3 (I)
```

80

```
        P4 (I) = (DEX (I) + 1. − GA (I)) * BK
7       Q4 (I) = LL (I) + RAN (I) * P4 (I)
        Y1 = FUN (Q1, N)
        Y2 = FUN (Q2, N)
        Y3 = FUN (Q3, N)
        Y4 = FUN (Q4, N)
        S1 = S1 + Y1 + Y2
        D1 = D1 + (Y1 − Y2) ** 2
        S2 = S2 + Y3 + Y4
        D2 = D2 + (Y1 + Y3 − Y2 − Y4) ** 2
        GO TO 5
3       EST1 = 0.5 * S1 / AKN
        ERR1 = 1.5 * DSQRT (D1) / AKN
        DEV1 = ERR1 * T
        EST2 = 0.25 * (S1 + S2) / AKN
        ERR2 = 0.75 * DSQRT (D2) / AKN
2       DEV2 = ERR2 * T * AK
        RESULT = 0.5 * (EST1 + EST2) * ABS (JAC)
        RETURN
        END
C
C
C       SUBROUTINE VOLT WHICH CALCULATES THE VOLTAGE MATRIX
C       VM
C
C       GEOMETRY IN THE Y−Z PLANE
C
C
        SUBROUTINE VOLT(F,THITA0,PHI0,A,B,V)
        REAL TSI,TCO,PS,PC,KY,KZ,A,B,K0,F,KX
        REAL MAR,GTI,PRS,PRC,MOD,KZHTA
        REAL S(1:230),T(1:230),PSI(1:230),LS(1:230),WI(1:230),THITA0,PHI0
        INTEGER NMAX
        COMPLEX V(1:230),J,STR,VOM
        COMMON/ BRAVO/ KX,KY,KZ
        COMMON/ RC2/ LS,WI,S,T,PSI
        COMMON/ RC1/ NMAX
        COSD(X)=COS(X*RAD)
        SIND(X)=SIN(X*RAD)
        PI=4.*ATAN(1.)
        RAD=PI/180.
        K0=PI*F/15.
        J=CMPLX(0.,1.)
        TSI=SIND(THITA0)
        TCO=COSD(THITA0)
        PS=SIND(PHI0)
        PC=COSD(PHI0)
        KY=K0*TSI*PS
        KX=K0*TSI*PC
        KZ=K0*TCO
        DO 234 K=1,NMAX
            PRS=SIND(PSI(K))
```

```fortran
      PRC=COSD(PSI(K))
      MAR=KY*S(K)+KZ*T(K)
      STR=CEXP(-J*MAR)
      VOM=(STR/SIN(LS(K)*K0))*(A*PRS+B*PRC)
      KZHTA=KY*PRS+KZ*PRC
      MOD=COS(K0*LS(K))-COS(KZHTA*LS(K))
      GTI=KZHTA**2-K0**2
      IF(ABS(KZHTA-K0)/K0.LT.1.E-2.OR.
     &       .ABS(KZHTA+K0)/K0.LT.1.E-2)THEN
      V(K)=VOM*LS(K)*SIN(K0*LS(K))
      ELSE
      V(K)=(2*K0/GTI)*VOM*MOD
      ENDIF
234   CONTINUE
      RETURN
      END
C
      SUBROUTINE CLUDCP (A, N, NP, INDX)
      INTEGER NP, N, INDX (NP), I, J, K, P, NMAX
      PARAMETER (NMAX = 230)
      COMPLEX  A (NP, NP), TEMP, ETA, W (NMAX)
      REAL AAMAX, DUM
      DO 1 K = 1, N-1
      AAMAX = CABS (A (K, K))
      P = K
      DO 2 I = K+1, N
      DUM = CABS (A (I, K))
      IF (DUM .GT. AAMAX) THEN
      AAMAX = DUM
      P = I
      END IF
2     CONTINUE
      INDX (K) = P
      DO 3 J = 1, N
      TEMP = A (K, J)
      A (K, J) = A (P, J)
      A (P, J) = TEMP
3     CONTINUE
      DO 4 J = K+1, N
      W (J) = A (K, J)
4     CONTINUE
      DO 5 I = K+1, N
      ETA = A (I, K) / A (K, K)
      A (I, K) = ETA
      DO 6 J = K+1, N
      A (I, J) = A (I, J) - ETA * W (J)
6     CONTINUE
5     CONTINUE
1     CONTINUE
      RETURN
      END
```

```
C
      SUBROUTINE CLUBSB (A, N, NP, INDX, X)
      INTEGER N, NP, I, J, INDX (NP), NMAX
      PARAMETER (NMAX = 230)
      COMPLEX A (NP, NP), X (NP), TEMP, Y (NMAX)
C
C     DO PERMUTATIONS ON THE EXCITATION VECTOR USING THE
C     INFORMATION ON THE ROW OPERATIONS DONE IN CLUDCP.
C
      DO 1 K = 1, N-1
      TEMP = X (K)
      X (K) = X (INDX (K))
      X (INDX (K)) = TEMP
   1  CONTINUE
C
C     FORWARD ELIMINATION
C
      DO 2 I = 1, N
      Y (I) = X (I)
      DO 2 J = 1, I-1
      Y (I) = Y (I) - A (I, J) * Y (J)
   2  CONTINUE

C
C     BACK SUBSTITUTION
C
      DO 3 I = N, 1, -1
      X (I) = Y (I)
      DO 4 J = I+1, N
      X (I) = X (I) - A (I, J) * X (J)
   4  CONTINUE
      X (I) = X (I) / A (I, I)
   3  CONTINUE
      RETURN
      END
C
C     SUBROUTINE RADIAT TO COMPUTE THE RADAR CROSS SECTION
C     OF A PLANAR STRUCTURE COMPOSED OF ARBITRARILY
C     ORIENTED PLANAR DIPOLES.
C
      SUBROUTINE RADIAT (F,THITA0,PHI0,NMAX,A,B,RCS)
      REAL RC,THITA0,PHI0,LS(1:230),WI(1:230),S(1:230),T(1:230),P1
      REAL CR,F,K0,PI,UN,DM,EM,RAD,P,R,A,B,THITA,PHI,RCS,PSI(1:230)
      REAL KX,KY,KZ,KRON,KG
      INTEGER G,NMAX
      COMPLEX J,NTHI0,NPHI0,TEMP1,TEMP2,CUR(1:230)
      COMMON/ BRAVO/ KX,KY,KZ
      COMMON/ RC2/ LS,WI,S,T,PSI
      COMMON/ RC4/ CUR
      COSD(X) = COS(X*RAD)
      SIND(X) = SIN(X*RAD)
```

```fortran
      PI = 4. * ATAN(1.)
      RAD = PI/180.
      K0 = PI*F/15.
      UN=120.*PI
      THITA =180.- THITA0
      PHI = 180. + PHI0
      J=CMPLX(0.,1.)
      TEMP1=(0.,0.)
      TEMP2=(0.,0.)
      NTHI0=(0.,0.)
      NPHI0=(0.,0.)
      DO 58 G=1,NMAX
        P1=PSI(G)
        DM=K0*(S(G)*SIND(THITA)*SIND(PHI)+T(G)*COSD(THITA))
        EM=K0*(SIND(P1)*SIND(THITA)*SIND(PHI)+
     &        +COSD(P1)*SIND(THITA))
        P=SIND(P1)*COSD(THITA)*SIND(PHI)-COSD(P1)*SIND(THITA)
        TEMP1=P*CEXP(J*DM)*CUR(G)/SIN(K0*LS(G))
        TEMP2=CEXP(J*DM)*CUR(G)*SIND(P1)*COSD(PHI)/SIN(K0*LS(G))
        IF(ABS(EM-K0)/K0.LT.1.E-2.OR.ABS(EM+K0)/K0.LT.1.E-2)THEN
        KG=LS(G)*SIN(K0*LS(G))
        ELSE
        KG=-2*K0*(COS(EM*LS(G))-COS(K0*LS(G)))/(EM**2-K0**2)
        ENDIF
        NTHI0=TEMP1*KG+NTHI0
        NPHI0=NPHI0+KG*TEMP2
58    CONTINUE
      CR=CABS(NTHI0)**2+CABS(NPHI0)**2
      KRON=(A*KY+B*KZ)/KX
      RC=(K0**2)*(UN**2)*CR/(4.*PI*(ABS(A)**2+ABS(B)**2+
     &      +ABS(KRON)**2))
      IF((RC/((30./F)**2)).LT.1.E-6)THEN
             RCS = 10.*ALOG10(1.E-6)
      ELSE
             RCS=10.*ALOG10(RC/((30./F)**2))
      ENDIF
      RETURN
      END
```

APPENDIX B

PROGRAM TREE

```
C                      PROGRAM TREE
C
C      PROGRAM TO GENERATE A PLANAR FRACTAL TREE WITH
C      REDUCTION FACTOR (COND) AND BRANCHING ANGLE THETA
C      WRITTEN BY T.R. NELSON, PhD, UNIVERSITY OF CALIFORNIA
C      SAN DIEGO, LA JOLLA, CA, 90293, AND MODIFIED BY
C      LT. JOHN DEMIRIS TO GENERATE THE INPUT DATA FOR
C      THE RCS PROGRAM.
C
C      INPUT DATA:
C
C      L = NUMBER OF BRANCHING LEVELS.
C      N = NUMBER OF BRANCH SEGMENTS.
C      ILEN = INITIAL LENGTH.
C      ISP = INITIAL STARTING POINT.
C      COND = REDUCTION FACTOR.
C      THETA = BRANCHING ANGLE.
C
C      OUTPUT DATA:
C
C      IX, IY = COORDINATES OF FIRST AND END POINT OF EACH
C               GENERATED BRANCH.
C      INPUT DATA FOR RCS PROGRAM
C
       REAL ZZ (1:5,1:1024),ISP,ILEN,IX,IY,ITH1
       OPEN (UNIT=1, FILE = 'INGEOM',FORM = 'FORMATTED')
       OPEN (UNIT=2, FILE = 'OUT', FORM = 'FORMATTED')
       OPEN (UNIT=10,FILE ='INPUT1',FORM='FORMATTED')
       READ(1,*,END=10) L,N,ILEN,ISP,COND,THETA
10     CLOSE(1)
       ZZ( 1,1) = ISP
       ZZ (4,1) = ILEN
       ZZ (3,1) = 0.
       ZL = ZZ (4,1)
       ZZ (2,1) = 0.
       ZN = N
       PI = 3.14159265
       IX = 0.
       IY = 0.-ILEN
       IX = ZZ(2,1)
       IY = ZZ(1,1)
       DO 100 LOOP =1,L
```

```
            ZLOOP = LOOP
            NPTS = N**ZLOOP
            INC = 0
            NPREV = N**(ZLOOP-1)
            PREV = NPREV
            ANGLE = (ZN-1.0)/2.0
            ZINDX = -ANGLE
            DO 200 J =1,NPTS
            ZJ = J
            IF (INC.GE.N) ZINDX=-ANGLE
            IF (INC.GE.N) INC=0
            IW=NPTS-J+1
            IR = PREV-ZJ/ZN+1.0
            ZL=ZZ(4,IR)
            T = ZZ(3,IR)
            X = ZZ(1,IR)
            Y = ZZ(2,IR)
            ZL1 = ZL*COND
            IF (ZL1.LT.0.1) GOTO 300
            TH1 = ZL1/33.0
            T1 = T+THETA*ZINDX
            ZZ(3,IW) = T1
            T2 = T1*PI/180.0
            IX = Y
            IY = X
            TEMPX1=IX
            TEMPY1=IY
C
C     IX,IY ARE THE COORDINATES OF THE FIRST POINT OF THE
C     BRANCH ALONG THE X,Y AXIS RESPECTIVELY
C
            WRITE(2,*) IX,IY
            X1 = ZL1*COS(T2)+X
            Y1 = ZL1*SIN(T2)+Y
            IX=Y1
            IY=X1
C
C     IX,IY ARE THE COORDINATES OF THE END POINT OF THE
C     BRANCH ALONG THE X,Y AXIS RESPECTIVELY
C
            WRITE(2,*) IX,IY
            TEMPX2=IX
            TEMPY2=IY
C
C     S AND T ARE THE COORDINATES OF THE CENTER OF EACH
C     BRANCH
C
            S = (TEMPX2+TEMPX1)/2.
            T = (TEMPY2+TEMPY1)/2.
            PSI1=ATAN((TEMPX2-TEMPX1)/(TEMPY2-TEMPY1))
            PSI=PSI1*180./PI
```

```
            ZLHALF=ZL1/2.
            TH1HALF=TH1/2
            WRITE(10,*) ZLHALF,TH1HALF,S,T,PSI
            ZZ(1,IW)=X1
            ZZ(2,IW)=Y1
            ZZ(4,IW)=ZL1
            ZINDX=ZINDX+1.0
            INC=INC+1
200         CONTINUE
100     CONTINUE
300     STOP
        END
```

LIST OF REFERENCES

1. Mandelbrot, B.B., *The Fractal Geometry of the Nature*, W.H. Freeman and Company, New York, 1983.

2. Harrington, R.F. , *Field Computation by Moment Methods*, Robert E. Krieger Company, Florida, 1968.

3. Stutzman, W.L. and Thiele, G.A., *Antenna Theory and Design*, John Wiley & Sons, Inc, 1981.

4. Balanis, C.A., *Antenna Theory and Design*, Harper & Row, Publishers, New York, 1982.

5. Newman, E.H., *Simple Examples of the Method of Moments in Electromagnetics*, IEEE Transactions on Education, Vol. 31, No. 3, pp. 193–199, August 1988.

6. Jakeman, E., *Scattering by Fractal Objects*, Nature, Vol. 307, No. 5946, pp. 110, 5–11 January 1984.

7. Nelson, T.R. and Manchester, D.K., *Modeling of Lung Morphogenesis Using Fractal Geometries*, IEEE Transactions on Medical Imaging, Vol. 7, No. 4, pp. 321–327, December 1988.

8. Harrington, R.F. and Mautz, J.R., *Straight Wires with Arbitrary Excitation and Loading*, IEEE Transactions on Antennas and Propagation, Vol. AP–15, No. 4, pp. 502–515, July 1967.

9. Janaswamy, R. and Lee, S.W., *Scattering from Dipoles Loaded with Diodes*, IEEE Transactions on Antennas and Propagation, Vol. AP–36, No. 11, pp. 1649–1651, November 1988.

INITIAL DISTRIBUTION LIST

1. Hellenic Navy General Staff   4
    Second Branch, Education Department
    Stratopedo Papagou, Cholargos
    Athens, Greece

2. Library, Code 0142   2
    Naval Postgraduate School
    Monterey, California 93943–5002

3. Defense Technical Information Center   2
    Cameron Station
    Alexandria, Virginia 22304–6145

4. Professor R. Janaswamy, Code 62JS   4
    Department of Electrical and Computer Engineering
    Naval Postgraduate School
    Monterey, California 93943

5. Professor M. A. Morgan, Code 62MW   1
    Department of Electrical and Computer Engineering
    Naval Postgraduate School
    Monterey, California 93943

6. Professor R. Hippenstiel, Code 62HI   1
    Department of Electrical and Computer Engineering
    Naval Postgraduate School
    Monterey, California 93943

7. Chairman, Code 62   1
    Department of Electrical and Computer Engineering
    Naval Postgraduate School
    Monterey, California 93943

8. John Demiris   2
    Ploutarchou 17, Marousi
    Athens, 22151, Greece

9. Grigorios Voulgarakis   1
   Thessalonikis 8, Cholargos
   Athens, 15562, Greece

10. Professor T.R. Nelson   1
    Department of Radiology
    University of California
    San Diego, La Jolla, California 92093